
**STOPPING
WATER POLLUTION
AT ITS SOURCE**

375EO
MISA
Quality



MISA

Municipal/Industrial Strategy for Abatement

**MODELLING OXYGEN DEPLETION IN
THE KAMINISTIQUIA RIVER
THUNDER BAY, ONTARIO**

SEPTEMBER 1988



**Environment
Ontario**

Jim Bradley
Minister

MODELLING OXYGEN DEPLETION IN THE KAMINISTIGUIA RIVER,
THUNDER BAY, ONTARIO

by

R.C. McCrimmon,¹ D.C.L. Lam,¹ S. Klose² and Z. Novak²

¹ Rivers Research Branch, National Water Research Institute,
Inland Waters Directorate, Environment Canada, Burlington, Ontario

² River Systems Section, Water Resources Branch,
Ontario Ministry of the Environment, Toronto, Ontario

September 1988

TABLE OF CONTENTS

	PAGE
FOREWORD	ii
ABSTRACT	iv
1. INTRODUCTION	1
2. GOALS AND OBJECTIVES	2
3. DO-BOD MODEL	2
4. DATA BASE	6
4.1 DO-BOD Model Calibration Data	6
4.2 Verification Data	7
5. RESULTS	8
5.1 Sodium Simulation Using the 3 Layer Box Model	8
5.2 DO-BOD Model Calibration	9
5.3 DYRESM Verification	13
5.4 DO-BOD Model Verification	14
5.5 DO-BOD Model Sensitivity Analysis	16
6. CONCLUSIONS	21
ACKNOWLEDGEMENT	24
REFERENCES	24
APPENDIX - FIGURES	

CONTENTS

Page

11	FOREWORD	
13	CHAPTER I	
15	CHAPTER II	15
18	CHAPTER III	18
22	CHAPTER IV	22
25	CHAPTER V	25
28	CHAPTER VI	28
32	CHAPTER VII	32
35	CHAPTER VIII	35
38	CHAPTER IX	38
42	CHAPTER X	42
45	CHAPTER XI	45
48	CHAPTER XII	48
52	CHAPTER XIII	52
55	CHAPTER XIV	55
58	CHAPTER XV	58
62	CHAPTER XVI	62
65	CHAPTER XVII	65
68	CHAPTER XVIII	68
72	CHAPTER XIX	72
75	CHAPTER XX	75
78	CHAPTER XXI	78
82	CHAPTER XXII	82
85	CHAPTER XXIII	85
88	CHAPTER XXIV	88
92	CHAPTER XXV	92
95	CHAPTER XXVI	95
98	CHAPTER XXVII	98
102	CHAPTER XXVIII	102
105	CHAPTER XXIX	105
108	CHAPTER XXX	108
112	CHAPTER XXXI	112
115	CHAPTER XXXII	115
118	CHAPTER XXXIII	118
122	CHAPTER XXXIV	122
125	CHAPTER XXXV	125
128	CHAPTER XXXVI	128
132	CHAPTER XXXVII	132
135	CHAPTER XXXVIII	135
138	CHAPTER XXXIX	138
142	CHAPTER XL	142
145	CHAPTER XLI	145
148	CHAPTER XLII	148
152	CHAPTER XLIII	152
155	CHAPTER XLIV	155
158	CHAPTER XLV	158
162	CHAPTER XLVI	162
165	CHAPTER XLVII	165
168	CHAPTER XLVIII	168
172	CHAPTER XLIX	172
175	CHAPTER L	175
178	CHAPTER LI	178
182	CHAPTER LII	182
185	CHAPTER LIII	185
188	CHAPTER LIV	188
192	CHAPTER LV	192
195	CHAPTER LVI	195
198	CHAPTER LVII	198
202	CHAPTER LVIII	202
205	CHAPTER LIX	205
208	CHAPTER LX	208
212	CHAPTER LXI	212
215	CHAPTER LXII	215
218	CHAPTER LXIII	218
222	CHAPTER LXIV	222
225	CHAPTER LXV	225
228	CHAPTER LXVI	228
232	CHAPTER LXVII	232
235	CHAPTER LXVIII	235
238	CHAPTER LXIX	238
242	CHAPTER LXX	242
245	CHAPTER LXXI	245
248	CHAPTER LXXII	248
252	CHAPTER LXXIII	252
255	CHAPTER LXXIV	255
258	CHAPTER LXXV	258
262	CHAPTER LXXVI	262
265	CHAPTER LXXVII	265
268	CHAPTER LXXVIII	268
272	CHAPTER LXXIX	272
275	CHAPTER LXXX	275
278	CHAPTER LXXXI	278
282	CHAPTER LXXXII	282
285	CHAPTER LXXXIII	285
288	CHAPTER LXXXIV	288
292	CHAPTER LXXXV	292
295	CHAPTER LXXXVI	295
298	CHAPTER LXXXVII	298
302	CHAPTER LXXXVIII	302
305	CHAPTER LXXXIX	305
308	CHAPTER LXXXX	308
312	CHAPTER LXXXXI	312
315	CHAPTER LXXXXII	315
318	CHAPTER LXXXXIII	318
322	CHAPTER LXXXXIV	322
325	CHAPTER LXXXXV	325
328	CHAPTER LXXXXVI	328
332	CHAPTER LXXXXVII	332
335	CHAPTER LXXXXVIII	335
338	CHAPTER LXXXXIX	338
342	CHAPTER LXXXXX	342
345	CHAPTER LXXXXXI	345
348	CHAPTER LXXXXXII	348
352	CHAPTER LXXXXXIII	352
355	CHAPTER LXXXXXIV	355
358	CHAPTER LXXXXXV	358
362	CHAPTER LXXXXXVI	362
365	CHAPTER LXXXXXVII	365
368	CHAPTER LXXXXXVIII	368
372	CHAPTER LXXXXXIX	372
375	CHAPTER LXXXXXX	375
378	CHAPTER LXXXXXXI	378
382	CHAPTER LXXXXXXII	382
385	CHAPTER LXXXXXXIII	385
388	CHAPTER LXXXXXXIV	388
392	CHAPTER LXXXXXXV	392
395	CHAPTER LXXXXXXVI	395
398	CHAPTER LXXXXXXVII	398
402	CHAPTER LXXXXXXVIII	402
405	CHAPTER LXXXXXXIX	405
408	CHAPTER LXXXXXXX	408
412	CHAPTER LXXXXXXXI	412
415	CHAPTER LXXXXXXXII	415
418	CHAPTER LXXXXXXXIII	418
422	CHAPTER LXXXXXXXIV	422
425	CHAPTER LXXXXXXXV	425
428	CHAPTER LXXXXXXXVI	428
432	CHAPTER LXXXXXXXVII	432
435	CHAPTER LXXXXXXXVIII	435
438	CHAPTER LXXXXXXXIX	438
442	CHAPTER LXXXXXXX	442
445	CHAPTER LXXXXXXXI	445
448	CHAPTER LXXXXXXXII	448
452	CHAPTER LXXXXXXXIII	452
455	CHAPTER LXXXXXXXIV	455
458	CHAPTER LXXXXXXXV	458
462	CHAPTER LXXXXXXXVI	462
465	CHAPTER LXXXXXXXVII	465
468	CHAPTER LXXXXXXXVIII	468
472	CHAPTER LXXXXXXXIX	472
475	CHAPTER LXXXXXXX	475
478	CHAPTER LXXXXXXXI	478
482	CHAPTER LXXXXXXXII	482
485	CHAPTER LXXXXXXXIII	485
488	CHAPTER LXXXXXXXIV	488
492	CHAPTER LXXXXXXXV	492
495	CHAPTER LXXXXXXXVI	495
498	CHAPTER LXXXXXXXVII	498
502	CHAPTER LXXXXXXXVIII	502
505	CHAPTER LXXXXXXXIX	505
508	CHAPTER LXXXXXXX	508
512	CHAPTER LXXXXXXXI	512
515	CHAPTER LXXXXXXXII	515
518	CHAPTER LXXXXXXXIII	518
522	CHAPTER LXXXXXXXIV	522
525	CHAPTER LXXXXXXXV	525
528	CHAPTER LXXXXXXXVI	528
532	CHAPTER LXXXXXXXVII	532
535	CHAPTER LXXXXXXXVIII	535
538	CHAPTER LXXXXXXXIX	538
542	CHAPTER LXXXXXXX	542
545	CHAPTER LXXXXXXXI	545
548	CHAPTER LXXXXXXXII	548
552	CHAPTER LXXXXXXXIII	552
555	CHAPTER LXXXXXXXIV	555
558	CHAPTER LXXXXXXXV	558
562	CHAPTER LXXXXXXXVI	562
565	CHAPTER LXXXXXXXVII	565
568	CHAPTER LXXXXXXXVIII	568
572	CHAPTER LXXXXXXXIX	572
575	CHAPTER LXXXXXXX	575
578	CHAPTER LXXXXXXXI	578
582	CHAPTER LXXXXXXXII	582
585	CHAPTER LXXXXXXXIII	585
588	CHAPTER LXXXXXXXIV	588
592	CHAPTER LXXXXXXXV	592
595	CHAPTER LXXXXXXXVI	595
598	CHAPTER LXXXXXXXVII	598
602	CHAPTER LXXXXXXXVIII	602
605	CHAPTER LXXXXXXXIX	605
608	CHAPTER LXXXXXXX	608
612	CHAPTER LXXXXXXXI	612
615	CHAPTER LXXXXXXXII	615
618	CHAPTER LXXXXXXXIII	618
622	CHAPTER LXXXXXXXIV	622
625	CHAPTER LXXXXXXXV	625
628	CHAPTER LXXXXXXXVI	628
632	CHAPTER LXXXXXXXVII	632
635	CHAPTER LXXXXXXXVIII	635
638	CHAPTER LXXXXXXXIX	638
642	CHAPTER LXXXXXXX	642
645	CHAPTER LXXXXXXXI	645
648	CHAPTER LXXXXXXXII	648
652	CHAPTER LXXXXXXXIII	652
655	CHAPTER LXXXXXXXIV	655
658	CHAPTER LXXXXXXXV	658
662	CHAPTER LXXXXXXXVI	662
665	CHAPTER LXXXXXXXVII	665
668	CHAPTER LXXXXXXXVIII	668
672	CHAPTER LXXXXXXXIX	672
675	CHAPTER LXXXXXXX	675
678	CHAPTER LXXXXXXXI	678
682	CHAPTER LXXXXXXXII	682
685	CHAPTER LXXXXXXXIII	685
688	CHAPTER LXXXXXXXIV	688
692	CHAPTER LXXXXXXXV	692
695	CHAPTER LXXXXXXXVI	695
698	CHAPTER LXXXXXXXVII	698
702	CHAPTER LXXXXXXXVIII	702
705	CHAPTER LXXXXXXXIX	705
708	CHAPTER LXXXXXXX	708
712	CHAPTER LXXXXXXXI	712
715	CHAPTER LXXXXXXXII	715
718	CHAPTER LXXXXXXXIII	718
722	CHAPTER LXXXXXXXIV	722
725	CHAPTER LXXXXXXXV	725
728	CHAPTER LXXXXXXXVI	728
732	CHAPTER LXXXXXXXVII	732
735	CHAPTER LXXXXXXXVIII	735
738	CHAPTER LXXXXXXXIX	738
742	CHAPTER LXXXXXXX	742
745	CHAPTER LXXXXXXXI	745
748	CHAPTER LXXXXXXXII	748
752	CHAPTER LXXXXXXXIII	752
755	CHAPTER LXXXXXXXIV	755
758	CHAPTER LXXXXXXXV	758
762	CHAPTER LXXXXXXXVI	762
765	CHAPTER LXXXXXXXVII	765
768	CHAPTER LXXXXXXXVIII	768
772	CHAPTER LXXXXXXXIX	772
775	CHAPTER LXXXXXXX	775
778	CHAPTER LXXXXXXXI	778
782	CHAPTER LXXXXXXXII	782
785	CHAPTER LXXXXXXXIII	785
788	CHAPTER LXXXXXXXIV	788
792	CHAPTER LXXXXXXXV	792
795	CHAPTER LXXXXXXXVI	795
798	CHAPTER LXXXXXXXVII	798
802	CHAPTER LXXXXXXXVIII	802
805	CHAPTER LXXXXXXXIX	805
808	CHAPTER LXXXXXXX	808
812	CHAPTER LXXXXXXXI	812
815	CHAPTER LXXXXXXXII	815
818	CHAPTER LXXXXXXXIII	818
822	CHAPTER LXXXXXXXIV	822
825	CHAPTER LXXXXXXXV	825
828	CHAPTER LXXXXXXXVI	828
832	CHAPTER LXXXXXXXVII	832
835	CHAPTER LXXXXXXXVIII	835
838	CHAPTER LXXXXXXXIX	838
842	CHAPTER LXXXXXXX	842
845	CHAPTER LXXXXXXXI	845
848	CHAPTER LXXXXXXXII	848
852	CHAPTER LXXXXXXXIII	852
855	CHAPTER LXXXXXXXIV	855
858	CHAPTER LXXXXXXXV	858
862	CHAPTER LXXXXXXXVI	862
865	CHAPTER LXXXXXXXVII	865
868	CHAPTER LXXXXXXXVIII	868
872	CHAPTER LXXXXXXXIX	872
875	CHAPTER LXXXXXXX	875
878	CHAPTER LXXXXXXXI	878
882	CHAPTER LXXXXXXXII	882
885	CHAPTER LXXXXXXXIII	885
888	CHAPTER LXXXXXXXIV	888
892	CHAPTER LXXXXXXXV	892
895	CHAPTER LXXXXXXXVI	895
898	CHAPTER LXXXXXXXVII	898
902	CHAPTER LXXXXXXXVIII	902
905	CHAPTER LXXXXXXXIX	905
908	CHAPTER LXXXXXXX	908
912	CHAPTER LXXXXXXXI	912
915	CHAPTER LXXXXXXXII	915
918	CHAPTER LXXXXXXXIII	918
922	CHAPTER LXXXXXXXIV	922
925	CHAPTER LXXXXXXXV	925
928	CHAPTER LXXXXXXXVI	928
932	CHAPTER LXXXXXXXVII	932
935	CHAPTER LXXXXXXXVIII	935
938	CHAPTER LXXXXXXXIX	938
942	CHAPTER LXXXXXXX	942
945	CHAPTER LXXXXXXXI	945
948	CHAPTER LXXXXXXXII	948
952	CHAPTER LXXXXXXXIII	952
955	CHAPTER LXXXXXXXIV	955
958	CHAPTER LXXXXXXXV	958
962	CHAPTER LXXXXXXXVI	962
965	CHAPTER LXXXXXXXVII	965
968	CHAPTER LXXXXXXXVIII	968
972	CHAPTER LXXXXXXXIX	972
975	CHAPTER LXXXXXXX	975
978	CHAPTER LXXXXXXXI	978
982	CHAPTER LXXXXXXXII	982
985	CHAPTER LXXXXXXXIII	985
988	CHAPTER LXXXXXXXIV	988
992	CHAPTER LXXXXXXXV	992
995	CHAPTER LXXXXXXXVI	995
998	CHAPTER LXXXXXXXVII	998
1002	CHAPTER LXXXXXXXVIII	1002
1005	CHAPTER LXXXXXXXIX	1005
1008	CHAPTER LXXXXXXX	1008
1012	CHAPTER LXXXXXXXI	1012
1015	CHAPTER LXXXXXXXII	1015
1018	CHAPTER LXXXXXXXIII	1018
1022	CHAPTER LXXXXXXXIV	1022
1025	CHAPTER LXXXXXXXV	1025
1028	CHAPTER LXXXXXXXVI	1028
1032	CHAPTER LXXXXXXXVII	1032
1035	CHAPTER LXXXXXXXVIII	1035
1038	CHAPTER LXXXXXXXIX	1038
1042	CHAPTER LXXXXXXX	1042
1045	CHAPTER LXXXXXXXI	1045
1048	CHAPTER LXXXXXXXII	1048
1052	CHAPTER LXXXXXXXIII	1052
1055	CHAPTER LXXXXXXXIV	1055
1058	CHAPTER LXXXXXXXV	1058
1062	CHAPTER LXXXXXXXVI	1062
1065	CHAPTER LXXXXXXXVII	1065
1068	CHAPTER LXXXXXXXVIII	1068
1072	CHAPTER LXXXXXXXIX	1072
1075	CHAPTER LXXXXXXX	1075
1078	CHAPTER LXXXXXXXI	1078
1082	CHAPTER LXXXXXXXII	1082
1085	CHAPTER LXXXXXXXIII	1085
1088	CHAPTER LXXXXXXXIV	1088
1092	CHAPTER LXXXXXXXV	1092
1095	CHAPTER LXXXXXXXVI	1095
1098	CHAPTER LXXXXXXXVII	1098
1102	CHAPTER LXXXXXXXVIII	1102
1105	CHAPTER LXXXXXXXIX	1105
1108	CHAPTER LXXXXXXX	1108
1112	CHAPTER LXXXXXXXI	1112
1115	CHAPTER LXXXXXXXII	1115
1118	CHAPTER LXXXXXXXIII	1118
1122	CHAPTER LXXXXXXXIV	1122
1125	CHAPTER LXXXXXXXV	1125
1128	CHAPTER LXXXXXXXVI	1128
1132	CHAPTER LXXXXXXXVII	1132
1135	CHAPTER LXXXXXXXVIII	1135
1138	CHAPTER LXXXXXXXIX	1138
1142	CHAPTER LXXXXXXX	1142
1145	CHAPTER LXXXXXXXI	1145
1148	CHAPTER LXXXXXXXII	1148
1152	CHAPTER LXXXXXXXIII	1152
1155	CHAPTER LXXXXXXXIV	1155
1158	CHAPTER LXXXXXXXV	1158
11		

FOREWORD

The study of the Kaministiquia River, originally planned as a waste assimilation capacity investigation in 1985, was subsequently expanded and included as a Municipal Industrial Strategy for Abatement (MISA) pilot site. Inclusion of the MISA objectives for the site study expanded the range of investigation from traditional nutrient and oxygen consuming waste concerns to include all known and suspected contaminants from point source dischargers to the river.

Part 1 of the Kaministiquia River water quality study presented the findings of water quality surveys carried out in 1986 as they relate to the assimilative capacity of the lower river. The findings focussed on the impact of oxygen consuming wastes. A traditional one-dimensional riverine model was utilized to define the dissolved oxygen depletion.

Part 2 of this series presented the findings on the thermal structure and hydrodynamics of the river based on a joint study between the Ontario Ministry of the Environment and Environment Canada.

This report, which is Part 3 in this series, presents the findings on oxygen depletion in the river based on further work of the joint study between the Ontario Ministry of the Environment and Environment Canada. The waste assimilation capacity of the lower river was evaluated utilizing two-dimensional estuary modelling techniques. The findings focus on the impact of oxygen consuming wastes, and the detailed spatial distribution of oxygen.

An investigation of the impact of toxic organic and inorganic wastes is underway utilizing the estuary models and will be presented

in subsequent technical reports.

In addition to the MISA study activities, the entire Thunder Bay near shore area is under investigation as part of the Remedial Action Plan (RAP) process.

Note:

The Great Lakes Forest Products Company, which discharges to the lower Kaministiquia River, has had a change in corporate name since the writing of this report. The new name is, The Canadian Pacific Forest Products Company. All references to the former name in this report, should be changed as noted above.

ABSTRACT

A three layer DO-BOD box model was developed, calibrated and verified for the Kaministiquia River as part of the development of water quality models for the MISA program. The model accounts for BOD decay, BOD settling, reaeration, sediment oxygen demand, diffusion, heated effluent loadings and transport. Transport was calculated using the previously modified DYRESM model (McCrimmon et al. 1987) and accounts for the intrusion of cooler Lake Superior water which creates thermal stratification.

Reasonably good results with average relative errors of 20.6% and 18.6% for the calibration period of August 11-15, 1986 and the verification period of June 15-21, 1987, respectively, were achieved. Vertical diffusion rates required increases for model verification due, likely, to different physical conditions existing during the period. A better hydrodynamic model and more measurements of water levels and velocities are desired. It was found that the low dissolved oxygen levels are most sensitive to changes in BOD loadings and transport. To satisfy the provincial water quality objective of a minimum dissolved oxygen concentration of 5 (mg/L), the BOD loadings from the Great Lakes Forest Products Company would have required approximately a 75% reduction. Other management strategies were also tested with the model which could be run on an IBM PC/AT microcomputer or compatibles.

RÉSUMÉ

Un modèle de rivière à trois couches pour le calcul de l'OD et de la DBO a été mis au point, étalonné et vérifié pour la Kaministiquia dans le cadre de la création de modèles de qualité de l'eau pour la SMID. Le modèle représente la dégradation de la DBO, sa charge après sédimentation, la réaération, la demande en oxygène des sédiments, la diffusion, le volume d'effluents chauds et le transport. Le transport a été calculé à l'aide du modèle DYRESM précédemment modifié (McCrimmon et coll. 1987) et tient compte de la pénétration des eaux plus froides du lac Supérieur à l'origine de la stratification thermique.

Des résultats raisonnablement concluants (pourcentages moyens d'erreur relative de 20,6 % et de 18,6 % respectivement) ont été obtenus pour la période d'étalonnage du 11 au 15 août 1986 et la période de vérification du 15 au 21 juin 1987. Les taux de diffusion verticale ont dû être augmentés lors de la vérification du modèle, probablement à cause des conditions différentes qui prévalaient au cours de cette période. Un meilleur modèle hydrodynamique et un plus grand nombre de mesures des niveaux d'eau et des vitesses sont souhaitables. On a découvert que les endroits où le volume d'oxygène dissous était faible étaient les plus sensibles quand la charge en DBO et son transport subissaient des modifications. Pour atteindre l'objectif provincial de qualité de l'eau, soit une concentration minimale d'oxygène dissous de 5 mg/L, la DBO provenant de la Great Lakes Forest Products Company devrait être réduite d'environ 75 %. D'autres stratégies de gestion ont également été étudiées sur le modèle de simulation qui pourrait être exécuté sur un micro-ordinateur PC/AT IBM ou une machine compatible.

DISSOLVED OXYGEN MODEL FOR THE KAMINISTIGUIA RIVER, THUNDER BAY, ONTARIO

1. INTRODUCTION

The lower Kaministiquia River located near Thunder Bay, Ontario is subject to industrial pollutant loadings which often cause the river water quality, especially dissolved oxygen concentrations, to fall below desired levels (MOE 1972, 1988). The Great Lakes Forest Products Company operates the largest pulp and paper mill in Ontario which discharges to the Kaministiquia River approximately 10 km. upstream of Lake Superior (see Figure 1). Application of a riverine water quality model would normally be sufficient to determine viable solutions. However, the delta of the Kaministiquia River is unusual since cooler and cleaner Lake Superior water intrudes upstream along the river bottom, which creates a vertical thermal structure with a distinct thermocline similar to that observed in lakes. This phenomenon also results in both a horizontal and a vertical gradient of dissolved oxygen concentration since the polluted water is warmer and flows downstream nearer the surface. Therefore, a river water quality model that accounts for vertically varying concentrations is required.

In a previous study (McCrimmon et. al. 1987) flow characteristics and water temperatures were determined for August 11-15, 1986 using a modified version of the one-dimensional dynamic reservoir simulation model, DYRESM. The river was divided into 16 connected segments which were simulated in turn using DYRESM in six-hour time steps. In this study a 3 layer 16 segment DO-BOD box model,

which uses the previously determined flows and water temperatures, was developed and calibrated for the 1986 data. In addition, data for June 15-21, 1987 was obtained and used to verify the DYRESM and DO-BOD models.

2. GOALS AND OBJECTIVES

The overall goal of the Kaministiquia River Water Quality Modelling Study is to develop and verify water quality models with predictive capability for the assessment of possible management strategies for the Municipal Industrial Strategy for Abatement (MISA) program on pollution control for rivers of the same type. The goals and objectives of the MISA program were laid out in a White Paper from MOE (MOE 1986). The objective of this study is to develop a Dissolved Oxygen - Biochemical Oxygen Demand (DO-BOD) model incorporating not only the multi-source, heated effluent conditions but also the modulations on the DO-BOD concentrations by the intrusion of the relatively cooler and denser lake water.

The present report describes (i) the DO-BOD model, (ii) the DO-BOD model calibration results, and (iii) the verification results of the DYRESM and DO-BOD models using the 1987 data. Also presented is a sensitivity analysis of DO and BOD to changes in model parameters, boundary conditions and loadings.

3. DO-BOD MODEL

The method for predicting DO and BOD concentrations involves a number of sequential steps, the results of which are used in ensuing

steps. A flowchart outlining these steps is presented in Figure 2(a). Basically, the steps involved are 1) predict water temperatures and flow characteristics using DYRESM, 2) calculate the equivalent box temperatures and transport for use in the DO-BOD 3 layer box model, 3) calculate the required diffusion rates for temperature using the box model, 4) check transport and diffusion using the box model to predict sodium, and 5) predict DO and BOD.

The DO-BOD model developed predicts the DO and BOD concentrations of 3 layers for each of the 16 river segments for a total of 48 boxes. The selection of a 3 layer box model was based upon the temperature profiles which indicated the existence of a 1.5 m thick epilimnion and a hypolimnion below a depth of 4.5 m, on average. Also, in the upper and lower layers, the horizontal flows were all downstream and upstream, respectively. The middle layer then covers the thermocline region which includes the vertically varying horizontal velocity zero point. Thus, the DO-BOD model is a two-dimensional model.

As displayed in the schematic diagram of a typical surface box in Figure 2(b), the DO-BOD box model accounts for horizontal and vertical flow, BOD decay, reaeration, sediment oxygen demand, vertical diffusion, external loadings and BOD settling. Downstream of the first river reach the middle layer boxes often contained 10 to 20% upstream flow. Since only a net downstream flow is used in the model for the middle layer then a horizontal diffusion in the middle layer is included in an attempt to account for the neglected effects of upstream flow in the DO-BOD model.

The equations used in the DO-BOD model are

$$V \frac{dDO}{dt} = -u V \frac{dDO}{dx} + K_d V \frac{d^2 DO}{dz^2} - K_1 V \frac{BOD \cdot DO}{DO + C_H} + K_2 V (DO_S - DO) - SOD A_{sed} + DO_L \quad (1)$$

$$V \frac{dBOD}{dt} = -u V \frac{dBOD}{dx} + K_d V \frac{d^2 BOD}{dz^2} - K_1 V \frac{BOD \cdot DO}{DO + C_H} - W A BOD + BOD_L \quad (2)$$

and for the middle layer add the following

$$+ K_{EX} V \frac{d^2 C}{dx^2} \quad \text{where } C = DO \text{ for equation (1)}$$

$$C = BOD \text{ for equation (2)}$$

where

V = box volume (m^3)

BOD = biochemical oxygen demand (g/m^3)

DO = dissolved oxygen concentration (g/m^3)

t = time (d^{-1})

u = horizontal velocity (m/d)

x = horizontal distance (m)

z = depth (m)

K_d = vertical diffusion constant (m^2/d)

K_1 = BOD decay rate (d^{-1})

C_H = half saturation constant (g/m^3)

$DO_S = 14.48 - 0.36T + 0.0043T^2$ = saturated [DO] (g/m^3)

T = water temperature of the top box (celcius)

K_2 = reaeration constant (d^{-1})

SOD = sediment oxygen demand ($g/m^2/d$)

A_{sed} = sediment surface area of box (m^2)

W = BOD settling rate (m/d)

A = horizontal area of box bottom (m^2)

DO_L = DO external loading (g/d)

BOD_L = BOD external loading (g/d)

K_{EX} = horizontal diffusion rate (m^2/d)

Through experimentation of different model equation solutions, a predictor-corrector method using a 1/2 hour time step was selected for the DO-BOD model. It should be noted that to conserve mass the flow rates from the DYRESM results had to be used explicitly. In more detail, the model equations were solved as follows:

for time step 1: explicit solution

$$\frac{C^{n+1} - C^n}{t} = f(C^n) \quad \text{where } C = \text{concentration}$$

n = time step level (n t=t)
t = time

for remaining time steps: 1) predictor

$$\frac{\tilde{C}^{n+1} - C^{n-1}}{2 t} = f(C^n)$$

2) corrector

$$\frac{C^{n+1} - C^n}{t} = f\left(\frac{\tilde{C}^{n+1} + C^n}{2}\right)$$

For each time step, the predictor calculation is performed on all boxes then the corrector is performed for all boxes to achieve the simulated values.

4. DATA BASE

Flow rates and water temperatures for August 11-15, 1986 were taken from the previous study (McCrimmon et. al. 1987). Other data required for calibration of the DO-BOD model, such as loadings and observations, were supplied by the Ontario Ministry of the Environment (MOE). The 1987 data used for verifying both the DYRESM and DO-BOD models was also supplied by MOE. In this section, the available data, calculated and estimated data and assumptions related to the data and model are presented for calibration and verification of the DO-BOD model and verification of the DYRESM model.

The Kaministiquia River is located in northern Ontario near Thunder Bay. The stretch of the river under investigation extends from the river outlet at Lake Superior to approximately 10 kilometres upstream, and includes the McKellar and Mission River branches, as depicted in Figure 1. The points A through P in Figure 1 indicate the cross-section locations at which parameter measurements were made by the MOE. By using these points and the added point Z, which is the location of the river's main pollutant source, as boundaries, 16 river sections were created for modelling purposes.

4.1 DO-BOD Model Calibration Data

The DO-BOD model was calibrated over the DYRESM calibration period of August 11-15, 1986. The flows, water temperature and hypsometric data were taken from the DYRESM calibration data base and results. The DO and BOD observations were supplied by MOE and included for most cross-sections 1) DO profiles at the right, middle and left

on August 15, 2) 4-hourly surface values of DO and BOD for August 11-14 and 3) hourly surface values of DO for August 11-14. At each cross-section the right, middle and left DO profiles were averaged. The river segment values were then estimated as the average of the upstream and downstream cross-section profiles. These profiles were used also as the initial conditions. Since there are no BOD observations below the surface, the initial values of the middle and bottom layers were assumed to be cleaner due to the upstream flow of water from Lake Superior and were set equal to the upstream concentration of 0.4 g/m^3 .

4.2 Verification Data

The DYRESM and DO-BOD models were verified over the period June 15-21, 1987. The water levels, velocity profiles and hypsometric data were taken from the 1986 data base. The DYRESM calibration data base was used for verification but with the following changes:

- 1) The 1987 values of daily Kakabeka Falls flow rates (for scaling velocity profiles), daily wind speed, daily air temperature, daily precipitation were inserted.
- 2) Daily wind directions were utilized instead of 6-hourly.
- 3) Estimated constant daily short wave radiation and vapour pressure were used.
- 4) The 1987 daily temperature profile observations were utilized, which were available at most cross-sections on each day, for initial conditions and simulation comparison.

The flow rates and water temperature required for the DO-BOD model

were taken from the DYRESM model. The average vertical diffusion rates required to obtain the desired box temperatures were calculated using the 3 layer box model. The DO observations consisted of daily profiles at most cross-sections. These were averaged to obtain river segment values for the initial conditions and for simulation comparison. The 1986 initial BOD values were used since there were no BOD observations for 1987.

5. RESULTS

The development of a calibrated and verified DO-BOD model for the lower Kaministiquia River involved, firstly, the simulation of flows and water temperatures using a modified version of DYRESM, secondly, the calculation of vertical diffusions for temperature using the 3 layer box model, thirdly, the simulation of sodium to check the transport processes of the 3 layer box model, and lastly, the application of the 3 layer box model for DO-BOD. In this section, the results of the above steps will be presented except for the calibration of DYRESM, which was presented previously (McCrimmon et. al. 1987).

5.1 Sodium Simulation Using the 3 Layer Box Model

The simulation of temperature using the 3 layer box model is a good test of the model and permits the calculation of diffusion rates. However, temperature is influenced by factors such as surface heat fluxes. Therefore, to truly test the transport of the model, especially with respect to loadings at the ZB diffuser, the simulation

of sodium (Na) was attempted. Na is relatively conservative and nonreactive and, like BOD, would be low in concentration if there was no loading from the diffuser.

Surface Na observations were available for 1986 for all cross-sections except for Z, E and N. Also, the effluent loadings from diffusers at ZB and BC were known (740 and 290 g/s respectively). Using the calculated temperature diffusion values in the model resulted in a mean relative error of 11.6%. In addition, all of the simulated values fell within the range of observations of each segment.

Since the diffusion rates of temperature and Na are likely different the values were varied to try to reduce the error. It was found that reducing the diffusion rates 50% for the diffuser segments and increasing the rates for the remaining segments 5 times decreased the mean relative error to 6.0%, while also maintaining the simulated values within the range of observations. These simulated values and the means and ranges of observations are plotted in Figure 3. The good results indicate the transport components of the 3 layer box model are reasonable. However, this testing of the model does not directly consider the two lower layers for which there are no sodium observations.

5.2 DO-BOD Model Calibration

The calibration of the DO-BOD model involved varying model parameters to minimize the difference between simulated and observed DO and BOD concentrations. Only diffusion rates and the biochemical,

as opposed to physical, parameters were considered.

The following values of the calibration parameters were found to result in the smallest differences between simulated and observed values.

$$\text{BOD decay rate} = 0.9 \text{ (d}^{-1}\text{)}$$

$$\text{Reaeration rate} = 0.05 \text{ (d}^{-1}\text{)}$$

$$\text{SOD rate} = 0.15 \text{ (g/m}^2\text{/d)}$$

$$\text{half saturation constant} = 1.5 \text{ (g/m}^3\text{)}$$

$$\text{horizontal diffusion rate} = 2.1 \times 10^6 \text{ (m}^2\text{/d)}$$

$$\text{diffusion at ZB, upper and lower interface} = 3.2 \times 10^{-2} \text{ (m}^2\text{/s)}$$

$$\text{diffusion at BC, upper interface} = 2.7 \times 10^{-4} \text{ (m}^2\text{/s)}$$

$$\text{lower interface} = 6.8 \times 10^{-5} \text{ (m}^2\text{/s)}$$

$$\text{diffusion at rest, upper and lower interface} = 0. \text{ (m}^2\text{/s)}$$

The resulting average relative error was 20.6% and is broken down for each layer and parameter in Table 1. The calibrated vertical diffusivities for the pollutants at ZB and BC are found to be 2.25 times the vertical thermal conductivities obtained using the computed temperature. The vertical diffusivities at the other segments were very small ($< 10^{-6}$) and, therefore, a value of zero was used. The simulated and observed values for the top and bottom layers for the last three days of the simulation period are shown in Figures 4 and 5. It can be seen in these Figures that the model predicts the horizontal variability of DO and BOD quite well.

Included in Figures 4 and 5 for each segment are vertical bars above and below the simulated values representing DO source and sink components, respectively, summed over the previous 6 hours. The

TABLE 1. MEAN RELATIVE ERRORS

	1986 CALIBRATION DATA	1987 VERIFICATION DATA
[DO] TOP LAYER	18.5%	18.6%
MIDDLE LAYER	36.2%	24.9%
BOTTOM LAYER	6.2%	11.7%
[BOD] TOP LAYER	23.7%	-
AVERAGE	20.6%	18.6%
TEMPERATURE	5.8%	5.9%

unshaded areas represent the source of DO from reaeration for the top layer but is indistinguishable in Figure 4 because of the small reaeration coefficient. The unshaded area represents the source from external loadings in the bottom layer in Figure 5. The darkest shaded areas represent the change in DO due to transport. In Figure 4, the transport is shown to be a large source of DO in the top layer of the upper segments. This is a result of the relatively higher upstream [DO]. The area shaded with right to left rising lines represents the change in DO due to diffusion. The diffusion components in Figures 4 and 5 are largest at the diffuser segments and indicate DO is diffusing out of the more oxygen-rich top layer into the more polluted bottom layers. The diffusion rates for the non-diffuser segments were set to zero so no diffusion is evident for these segments in 1986. The fourth component displayed represents BOD decay and SOD and, therefore, is always a sink of DO and is at the bottom of the vertical bars in Figures 4 and 5. This component is the dominant sink of DO and

is due mainly to decay since the SOD rate is relatively small.

The time series of DO and BOD at the surface of each segment are plotted in Figures 6 and 7, respectively, with observations at the upstream and downstream cross-sections included. In general, the DO and BOD fit the observations but short time scale variations are not reproduced by the model due mainly to the daily time step resolution of DYRESM. This is evident for segment LM in Figure 6, for example. Due to relatively high upstream concentrations of DO, low upstream concentrations of BOD and higher flow rates during the first half of the calibration period, the DO levels are higher and the BOD levels are lower as especially evident at ZB. This shows the importance of the flow characteristics on the DO-BOD levels. The substantial difference between the observed and simulated BOD at ZB on August 11 could be due to insufficient vertical transport or diffusion of BOD from the diffuser. However, it is more likely due to overestimating the flow rate on August 11, which was estimated to be twice as large as the subsequent days based upon the flows at Kakabeka Falls.

A three-dimensional representation of the study area with concentrations indicated by different shadings is represented for DO and BOD for August 15, 1986 in Figure 8. This figure shows that the polluted water discharged at the bottom of segment ZB generally flows in an upward and downstream direction and, due to the time dependent decay of BOD, the minimum [DO] occurs in the surface layer between segments EF, HI and JK. Downstream of JK the BOD levels are lower due to decay so that flow from the lower layers, diffusion and reaeration cause a slight increase in DO levels. Also evident is upstream flow of polluted water into the bottom layer of AZ from ZB. The cross-sectional area of the bottom layer at A is small, due to the rivers

shallowness at this point, so there is little flushing flow from upstream, which keeps the [DO] low and the [BOD] high. However, it should be noted that a lack of velocity measurements in this area precludes the assumption that there is upstream flow of polluted water into AZ.

5.3 DYRESM Verification

The data base used for verifying DYRESM from June 15-21, 1987 was outlined in Section 4. The major differences from the calibration data base are the differing flows and meteorological conditions. Also, there are more observations, especially in the lower layers, than in 1986. The remaining model parameters were the same as the 1986 data.

The first simulations of the Kaministiquia River using the verification data are plotted in Figure 9 for every other day. The simulated values compared reasonably well (root mean square error (rms) = 1.15°C and average relative error = 5.9%) with the observed profiles. These results are almost as good as the 1986 data calibrations (rms = 0.93°C and average relative error = 5.8%) which is encouraging since the 1987 observations are much more numerous and encompassing. The future acquisition of the daily solar radiation and vapour pressure could improve the simulations on a daily basis. The DYRESM model was assumed verified and no further parameter modifications were performed.

5.4 DO-BOD Model Verification

Verification of the DO-BOD 3 layer box model was attempted for the period June 15-21, 1987. The model inputs of flow and water temperature were taken from the DYRESM verification results and vertical diffusion values were recalculated using the 3 layer box model for temperature because the physical conditions changed. These inputs were then used in conjunction with the calibrated model parameter values, which were kept fixed, to verify the model.

The simulated DO values using the verification data were reasonably good with an average relative error of 18.6%. As seen in Table 1, this error is actually better than the calibrated error of 20.6% but the verified error is slightly biased to DO since no BOD observations were available. While the DO error for the bottom layer increased 5.5% for the verification simulations, the middle layer decreased 11.3%. The recalculated diffusion values used in the verification model are

$$\text{diffusion at ZB, upper interface} = 1.8 \times 10^{-4} \text{ (m}^2/\text{s)}$$

$$\text{lower interface} = 2.1 \times 10^{-3} \text{ (m}^2/\text{s)}$$

$$\text{diffusion at BC, upper interface} = 1.1 \times 10^{-4} \text{ (m}^2/\text{s)}$$

$$\text{lower interface} = 2.3 \times 10^{-5} \text{ (m}^2/\text{s)}$$

$$\text{diffusion at rest, upper interface} = 1.0 \times 10^{-4} \text{ (m}^2/\text{s)}$$

$$\text{lower interface} = 2.5 \times 10^{-5} \text{ (m}^2/\text{s)}$$

which correspond to 2.25 times the temperature rates at ZB and BC and 2.5 times the average temperature rates of the remaining segments. The simulated and observed DO and BOD values are plotted in Figures 4 and

5 for the last three days of the verification period. As compared to the 1986 observations, the [DO] in the bottom layer is evidently lower in 1987. This indicates that possibly the flow regime differs slightly from the 1986 period in that the upstream flow lake water intrusion along the river bottom does not extend as far upstream as in 1986. Also, the flow rates from August 12 to 15, 1986 ranged from 17.6 to 19.7 m³/s whereas they ranged from 21.2 to 23.2 from June 17 to 21, 1987, which suggests the varying flow regimes. The higher downstream flows of 1987 would likely push back the upstream intrusion of Lake Superior water, which could cause the observed decrease in DO at the bottom. For example, on the last day of the 1986 and 1987 periods the observed [DO] of the bottom layer at cross-section C was 6.9 (mg/l) in 1986 but was only 3.4 in 1987. This suggests less lake water, which was cleaner, reached cross-section C in 1987. It is possible that the water levels of the river and Lake Superior in 1987 are different from 1986 resulting in different velocity profiles.

The time series of the top layer DO and BOD concentrations for each segment are presented in Figures 6 and 7. As was the case for the 1986 plots, the verification simulated DO values generally fit the observations and indicate the lowest DO levels occur in the middle segments. When the flow rates increase on June 18, there is an increase in the [DO], as is evident especially for segments BC to EF in Figure 6. This correlation of higher DO concentrations with higher flow rates was also evident in the calibration simulations. Similarly, the BOD levels decrease June 18 because the upstream BOD values are lower and the BOD decay rates increase due to higher DO levels.

Three-dimensional representations of the rivers DO and BOD concentrations are presented in Figure 10. The pollutant loadings at ZB flow mostly vertically upwards and downstream as was seen for 1986 in Figure 8. The main difference from 1986 is that the [DO] of the lower layers is smaller in 1987 due mainly to increased diffusion rates, which cause DO to diffuse upwards to the less oxygen-rich layers.

5.5 DO-BOD Model Sensitivity Analysis

The sensitivity of DO and BOD concentrations to variations of model parameters and loadings was investigated using the 1986 data base. To standardize the sensitivity score, parameters and loadings were varied plus and minus 20%, one at a time, and the change in mean values of DO and BOD of each layer were recorded. The results of the analysis are presented in Table 2.

Table 2 is divided into 3 parts representing, first, the biochemical parameters, second, the loading and boundary conditions, and third, the diffusion rates. Of the biochemical parameters, DO and BOD are most sensitive to the BOD decay rate. The reaeration and SOD rates used in the model are at the lower end of normal values and do not noticeably effect DO and BOD when varied 20%. Reaeration and SOD rates that are 500% larger would not be unreasonable but, as seen in Table 2, such values result in a maximum relative change of only 3% (absolute change of +15% for the top layer [DO] when reaeration is increased 500%).

The large changes in DO and BOD displayed in the second part of Table 2 indicate the boundary conditions and BOD loading strongly

TABLE 2. DO-BOD MODEL SENSITIVITY ANALYSIS SUMMARY-
PERCENT CHANGE IN LAYER AVERAGE CONCENTRATION

	DECAY		REAERATION			C_H		SOD		
	+20%	-20%	+20%	-20%	+500%	+20%	-20%	+20%	-20%	+500%
TOP [DO]	-10	+13	+1	-1	+15	+4	-4	0	0	-2
MIDDLE [DO]	-5	+6	0	0	+1	+1	-2	0	0	-2
BOTTOM [DO]	-1	+2	0	0	0	0	0	0	0	-4
TOP [BOD]	-4	+6	0	0	-2	+2	-2	0	0	+1
MIDDLE [BOD]	-5	+7	0	0	0	+2	-2	0	0	+1
BOTTOM [BOD]	-4	+5	0	0	0	+1	-1	0	0	0

	BOD LOAD		DO LOAD		U/S [DO]		D/S [DO]	
	+20%	-20%	+20%	-20%	+20%	-20%	+20%	-20%
TOP [DO]	+17	-12	+1	-1	+19	-17	+23	-4
MIDDLE [DO]	+8	-7	0	0	+8	-8	+19	-11
BOTTOM [DO]	+1	-1	0	0	+1	-1	+15	-13
TOP [BOD]	-20	+22	0	0	-3	+4	-4	+1
MIDDLE [BOD]	-19	+21	0	0	-2	+3	-3	+1
BOTTOM [BOD]	-18	+18	0	0	-1	+1	-1	0

	K_{EX}		DIFF(ZB,BC) TEMP. Na(=TEMP/2)		DIFF(REST) TEMP. Na(=5*TEMP)	
	+20%	-20%	+20%	-20%	+20%	-20%
TOP [DO]	+2	-1	+2	+6	+10	+23
MIDDLE [DO]	+3	-3	-2	-5	-7	-13
BOTTOM [DO]	0	0	0	-1	-9	-27
TOP [BOD]	0	0	-5	-14	-6	-14
MIDDLE [BOD]	0	0	+4	+10	+3	+6
BOTTOM [BOD]	0	0	+22	+49	+4	+20

influence conditions in the river. The sensitivity of the boundary [BOD] was not investigated since the values were very small compared to the diffuser loadings. The combination of the sensitivity of DO and BOD to changes in the BOD decay rate and the BOD loadings, especially in the surface layer where the minimum [DO] occurs, clearly shows their importance. Also, the sensitivity to changes in the boundary concentrations and the insensitivity to changes in reaeration and SOD indicates the flow patterns are important.

In the third part of Table 2 the sensitivity results for diffusion rates are presented. The horizontal diffusion appears to have a small effect on layer concentrations. However, K_{EX} effects only the segments below the first branch so that the percent change in the layer average concentrations underestimates the effects of the horizontal diffusion on the lower segments. The vertical diffusion rates calculated for temperature and calibrated for sodium were used in the sensitivity analysis instead of plus or minus 20% (recall the calibrated DO-BOD model used (a) 2.25 times the temperature values for segments ZB and BC and (b) zero for the remaining segments). The [BOD] is sensitive to the diffuser diffusion rates because of the large concentration gradient in ZB and BC caused by the effluent loadings. The diffusion rates in the remaining segments affect both DO and BOD significantly because of the existing gradients resulting from the BOD decay and flow patterns.

A pie chart representing the relative effects of the three parts of Table 2 for the top layer is presented in Figure 11(a). The figure indicates all three components are important parts of the model. The pie chart in Figure 11(b) presents the relative importance of the kinetic coefficients (part 1 of Table 2). The values in Figure 11(b)

represent the absolute change in surface DO resulting from the change of each parameter from -20% to +20%. In Figure 11(b), the large areas of decay and half-saturation as compared to the remaining non-effluent dependent components of the model clearly displays the importance of the decay of the effluent loading.

The effects of changing the BOD loading were investigated in more detail since the DO levels were found to be very sensitive to varying effluent loadings. By reducing the BOD loading at the ZB diffuser in multiples of 10% of the original loading, the [DO] of the top and bottom layers of segments GJ on the last day of the calibration and verification periods were plotted in Figure 12. The top layer concentrations increased with decreased BOD loading, for both 1986 and 1987, as expected. The bottom layer concentration of GJ for 1986 was virtually unaffected by reduced BOD loading since the only transport into this box is from downstream. Conversely, the 1987 bottom concentration does change with changing loading. This effect is due to vertical diffusion, which was previously set to zero for the 1986 calibration simulations. Also indicated in Figure 12 is the amount of BOD reduction required to meet the provincial water quality objective (PWGO) of a minimum [DO] of 5 (mg/l). The load reduction required without changing other parameters would have been, approximately, 69% for 1986 and 74% for 1987. For example, when the BOD loading at ZB is reduced 80% then the resulting simulated DO concentrations, as depicted in Figure 13, are all above 5 (mg/l). Other management strategies, however, would have also been used, such as the use of oxygen diffusers and the adjustment of river flows and water levels. As an example of this strategy, an oxygen diffuser was hypothetically

used to insert 10,000 kg/d of DO throughout segment BC in the model. The DO concentrations at the end of the 1987 verification period, as simulated by the model, would then be as presented in Figure 14. At segment BC and downstream middle and upper layer boxes the DO concentrations are noticeably higher than the verification values, as previously presented in Figure 10. Though these DO levels are still below the PWQO for most segments, it is evident that there are other possible management strategies besides reducing loadings.

A plot similar to Figure 12 was made for segment AZ, which is the segment with the lowest simulated bottom layer [DO] and is presented in Figure 15. The top layer concentrations are relatively insensitive to BOD loading changes since they are dominated by flow from upstream. The bottom box of AZ is simulated as receiving most inflow from the ZB bottom box which receives Great Lakes Forest Products Company effluent loadings. Therefore, the AZ bottom box is very sensitive to the BOD loadings as evident in Figure 15. Note, however, that the surface box of GJ in Figure 12 reaches lower DO levels than the AZ bottom box but the required BOD reduction to achieve the PWQO of 5 (mg/l) in AZ is approximately the same (67% for 1986 and 77% for 1987) as for GJ. Also, as previously discussed, the upstream flow from ZB to AZ may not be as assumed in the model.

Monte Carlo simulations for BOD loading were carried out at different flow rates to better understand the probability of reaching certain minimum DO levels. The results of the simulations are presented in Figure 16. The means and standard deviations of flow and BOD loading at the ZB diffuser were calculated using the data from the calibration and verification periods. Flow rates were set to five different values based on its mean and standard deviation (see Figure

16). At each of the five flow rates, the DO-BOD model was executed for 100 BOD loadings, which were generated to fit a normal distribution with the observed mean and standard deviation, for a total of 500 program runs. Each run used averaged 1986 and 1987 conditions (e.g. initial concentrations and diffusion rates) and lasted five days. The relative number of occurrences of certain DO concentrations at the surface box of segment GJ on the fifth day is indicated in Figure 16 by the horizontal bars. The results show that at lower flow rates the [DO] is lower and is also less affected by changing the BOD loading. Conversely, at higher flow rates the [DO] is (i) higher due to the higher supply rate of DO from upstream and (ii) is more sensitive to the BOD loading as indicated by the larger simulated range of DO. The importance of these results is that it appears that to remedy low DO levels the flow rates must be considered in addition to reduction of the BOD loadings.

6. CONCLUSIONS

A DO-BOD 3 layer box model utilizing a predictor-corrector solution method and a 1/2 hour time step was developed, calibrated for the period August 11-15, 1986 and verified for the period June 15-21, 1987. The modified DYRESM model, which was calibrated previously (McCrimmon et. al. 1987) and is used to calculate flows and water temperatures for the 3 layer box model, was also verified in this study.

Calibration of the DO-BOD model, which involved changes of the bio-chemical parameters and diffusion rates, resulted in an average

relative error of 20.6%. The lowest DO levels were simulated to occur in the surface layer between segments EF, HI and JK. In general, the spatial variability and areas of low DO were simulated well.

Verification of the DO-BOD model over the period June 15-21, 1987 required the application of the modified DYRESM to obtain the flows and water temperatures. This verification of DYRESM resulted in a root mean square error of 1.15^oC and an average relative error of 5.9%, which are very similar to the errors obtained in the calibration simulations and appear acceptable.

The flows and water temperatures from the DYRESM verification simulations were used for the DO-BOD model verification. The initial simulations using the calibrated parameter values resulted in reasonable values except for the bottom [DO], which ranged up to 3 g/m³ too high. Increasing the diffusion rates from the calibrated value of zero to 2.5 times the temperature calculated rates of all segments excluding the diffuser segments decreased the mean relative error to 18.6%, which is lower than the calibration error of 20.6%. The required increase of the diffusion rates is likely due to different velocity profiles in 1987 caused, for example, by different water levels, though no observations are available to investigate this possibility. This hypothesis is based on the DO observations of the lower layer, which indicate the upstream flow from Lake Superior did not extend as far upstream as in 1986. The DO-BOD model was considered verified but this should be approached with caution since there were no BOD observations during this period.

Reasonable simulations of DO, BOD and water temperature using the modified DYRESM model and the DO-BOD model indicate the models are useful. The recalibration of the diffusion rates in the DO-BOD model

during verification suggest the need for more observations of velocities and water levels and possibly the need for a better hydrodynamic model. Also, detailed information on the loading is needed since the BOD loading is the most sensitive part of the model.

ACKNOWLEDGEMENT

R.C. McCrimmon was supported by MOE through Department of Supply and Services Contract No. KW405-7-2009/01-SE.

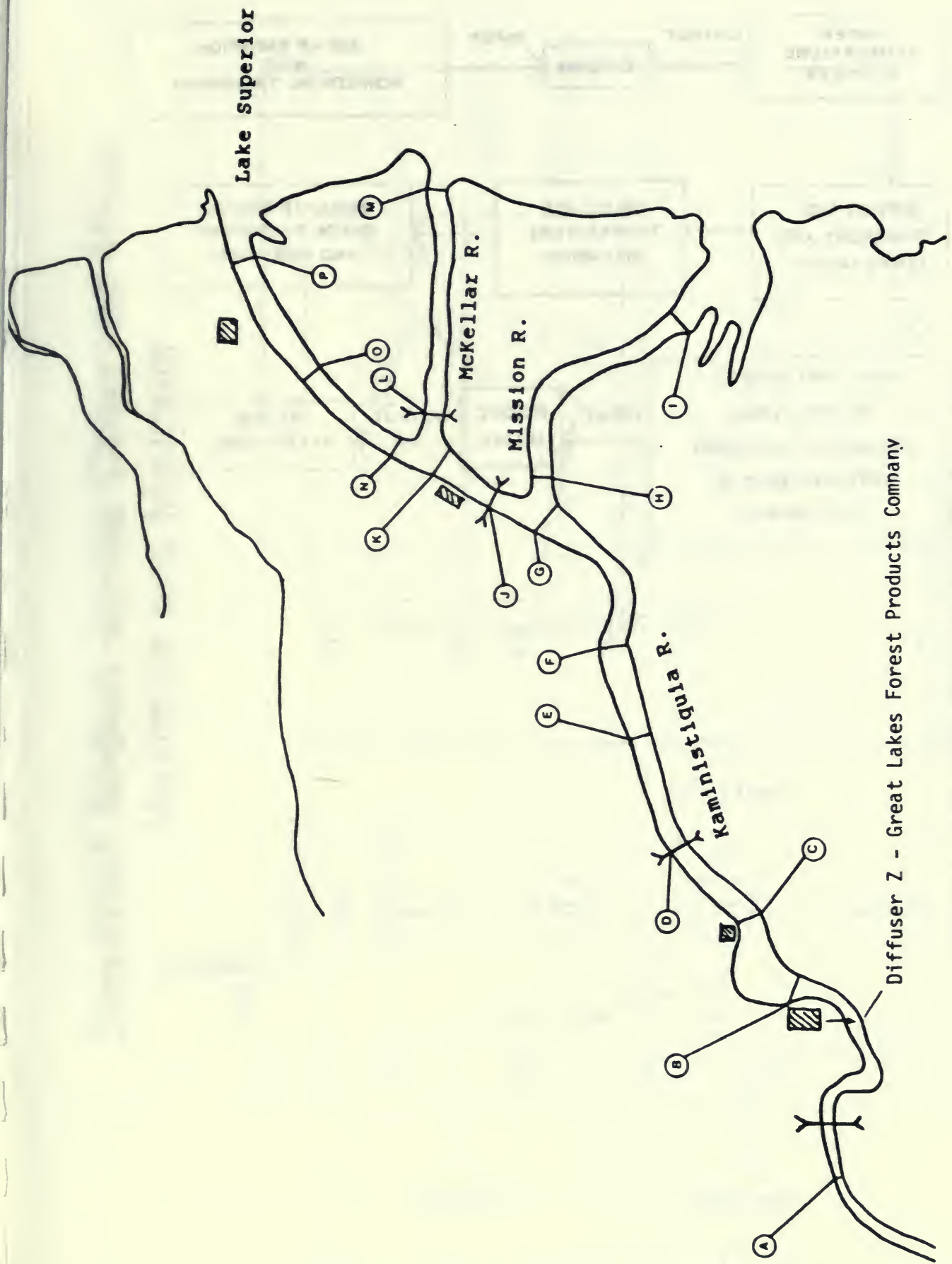
REFERENCES

- McCrimmon, R.C., Lam, D.C.L., Novak, Z., and Klose, S., 'Simulation of the Thermal Structure of Kaministiquia River, Thunder Bay, Ontario', NWRI Contribution #87-64, October 1987.
- MOE, 'Thunder Bay - Regional Water Quality Survey', September 1972.
- MOE, 'Water management; goals, policies, objectives and implementation procedures of the Ministry of the environment', 1978.
- MOE, 'Municipal-Industrial Strategy for Abatement, A Policy and Program Statement of the Government of Ontario on Controlling Municipal and Industrial Discharges into Surface Waters', June 1986.
- MOE, 'Kaministiquia River Water Quality Study, Part 1: Waste Assimilation Capacity', S.R. Klose, April 1988.

LIST OF FIGURES

FIGURE

1. The Lower Kaministiquia River Study Area
- 2(a). Model Flowchart
- 2(b). DO-BOD Model Schematic Diagram
3. Simulated Sodium and Observed Mean, Maximum and Minimum
4. Simulated and Observed Top Layer DO
5. Simulated and Observed Bottom Layer DO
6. Time Series of Top Layer DO
7. Time Series of Top Layer BOD
8. DO and BOD August 15, 1986 in 3-D
9. Simulated and Observed Temperature Profiles, 1987
10. DO and BOD June 21, 1987 in 3-D
- 11(a). Relative Sensitivities in %: Loadings, transport and kinetics
- 11(b). Sensitivity of Kinetic Coefficients
12. Response of DO at GJ to BOD Loading Changes
13. DO in 3-D June 21, 1987 with 80% BOD Load Reduction from ZB
14. DO in 3-D June 21, 1987 with 10,000 kg/d DO Diffused into Segment BC
15. Response of DO at AZ to BOD Loading Changes
16. Monte Carlo Simulations for BOD Loading



Diffuser Z - Great Lakes Forest Products Company

Figure 1. The Lower Kaministiquia River Study Area

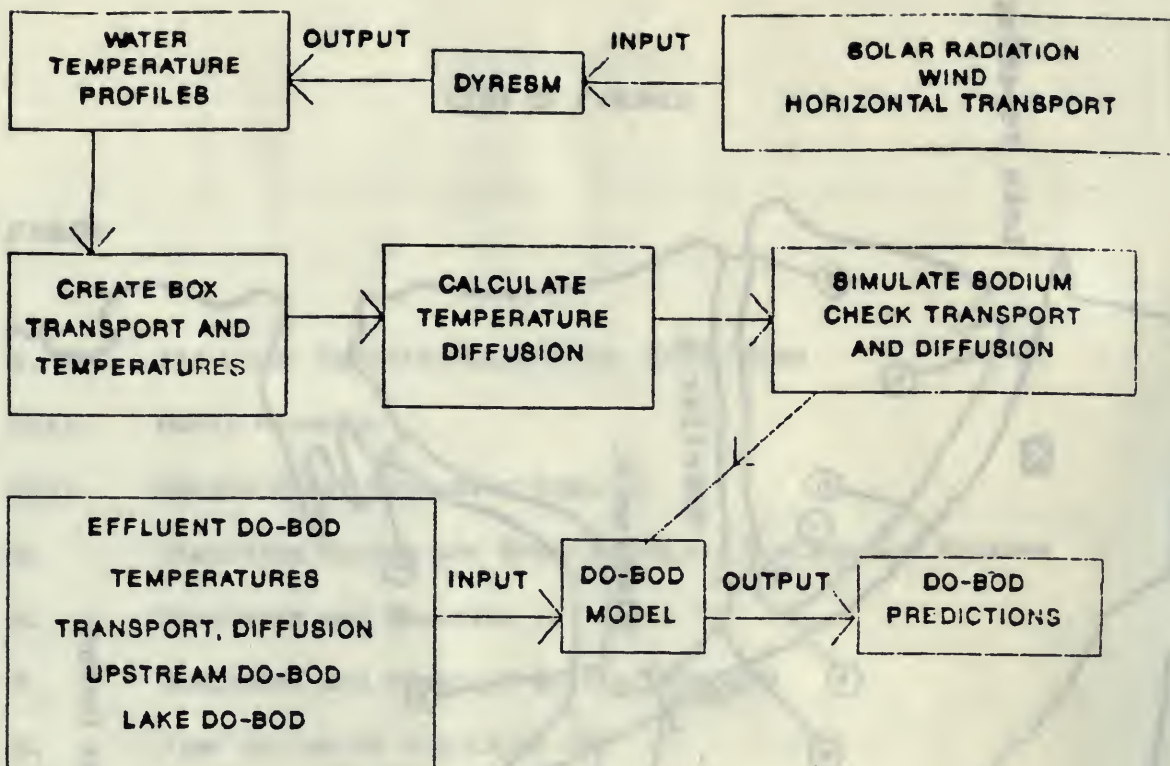


FIGURE 2(a). MODEL FLOWCHART

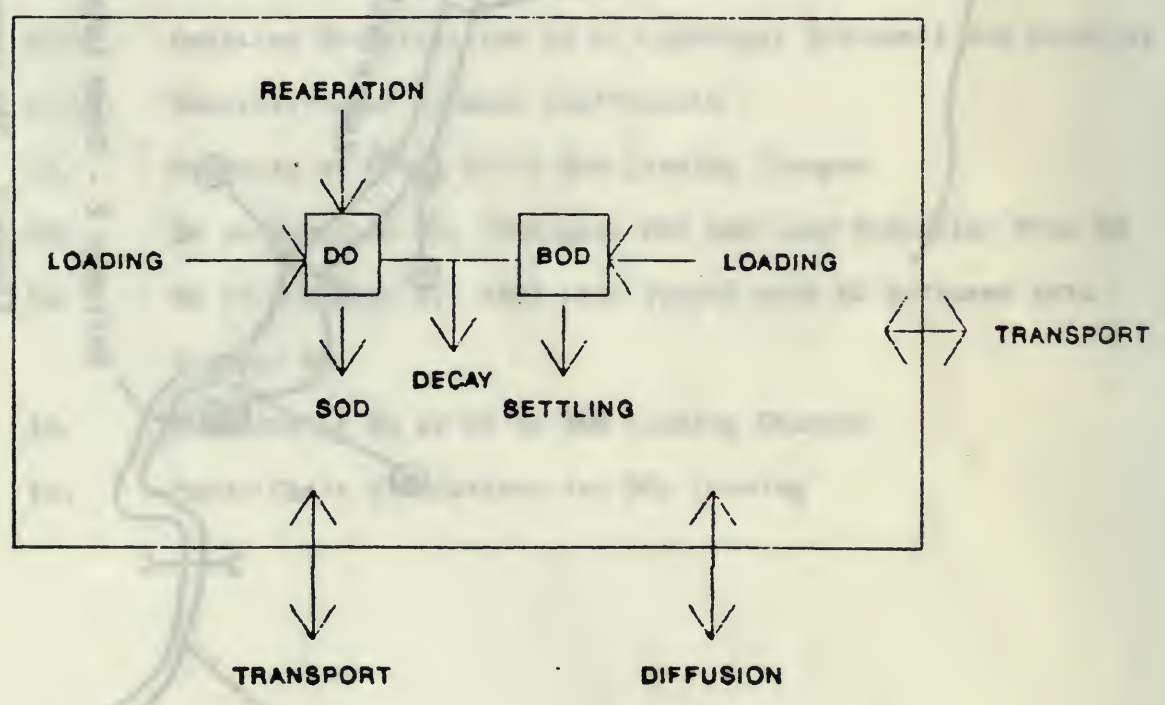


FIGURE 2(b). DO-BOD SCHEMATIC DIAGRAM

Simulated Sodium versus Observed Mean, Maximum and Minimum

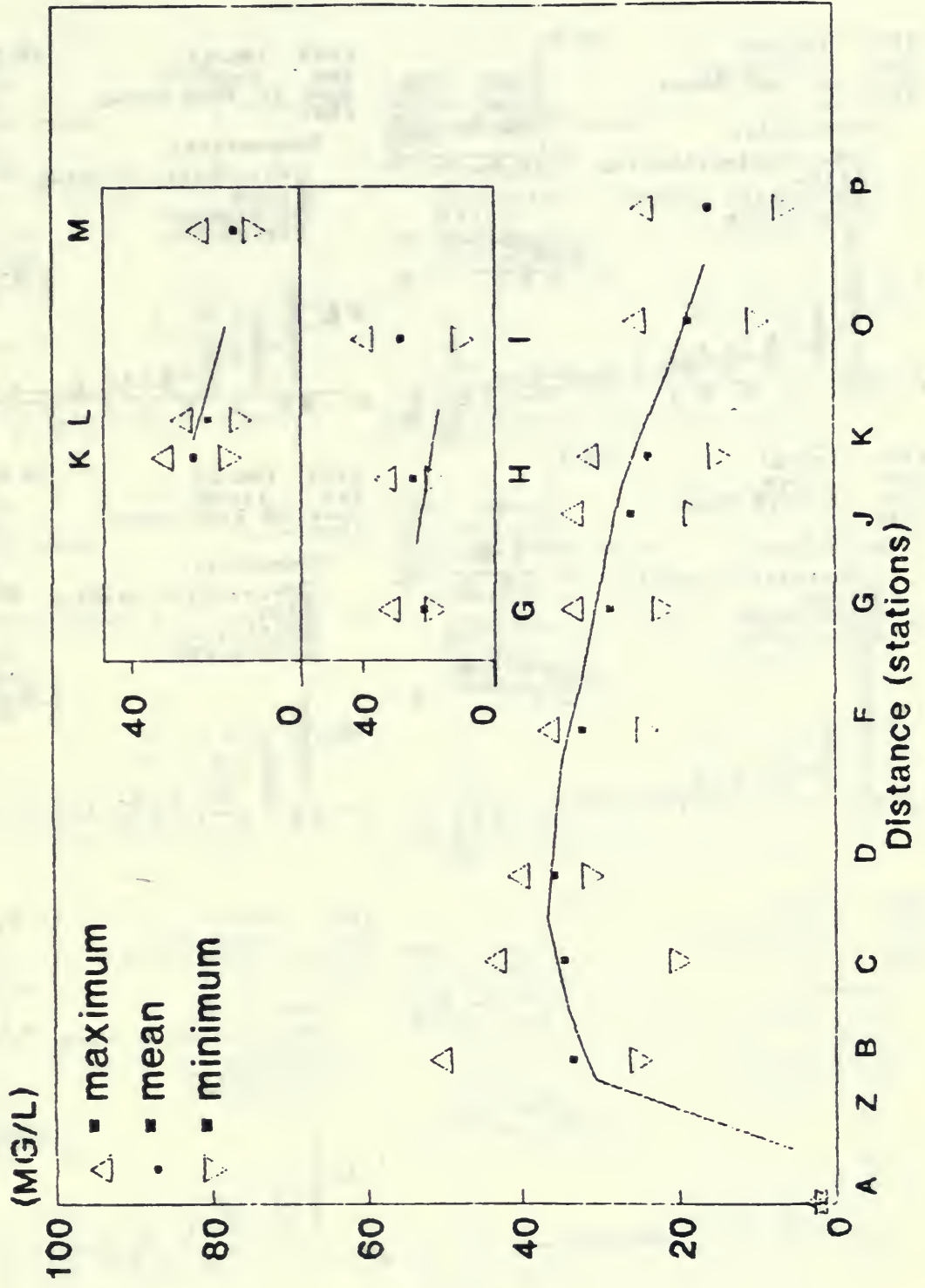
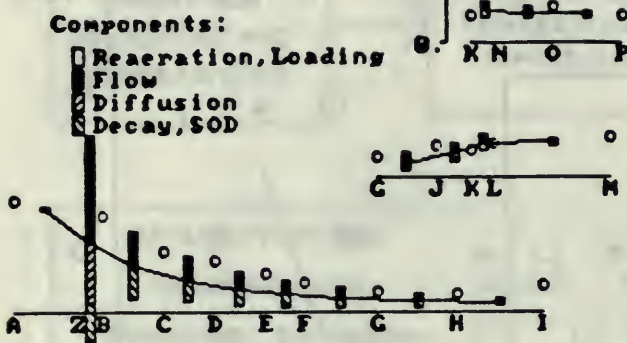
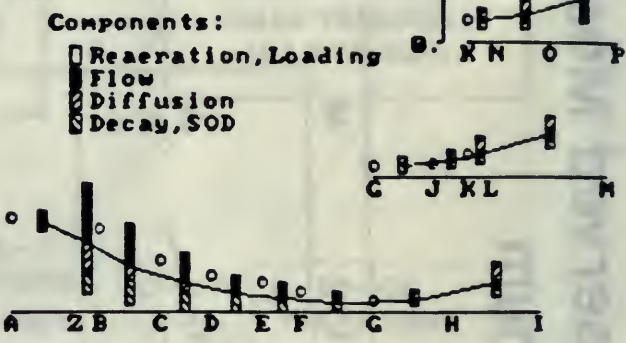


Figure 3.

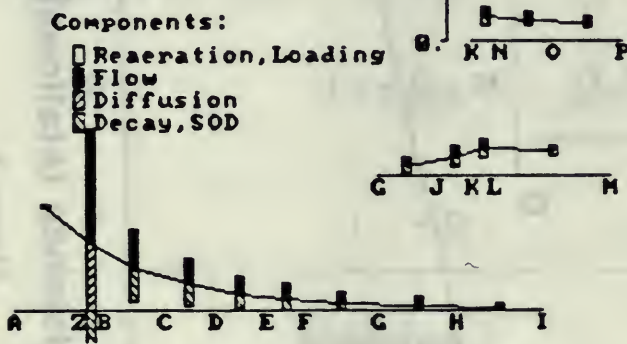
[DO] (MG/L)
top layer
Aug. 13 2400 hours
1986



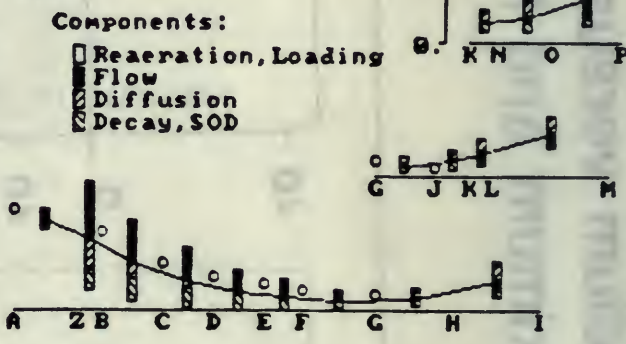
[DO] (MG/L)
top layer
June 19 2400 hours
1987



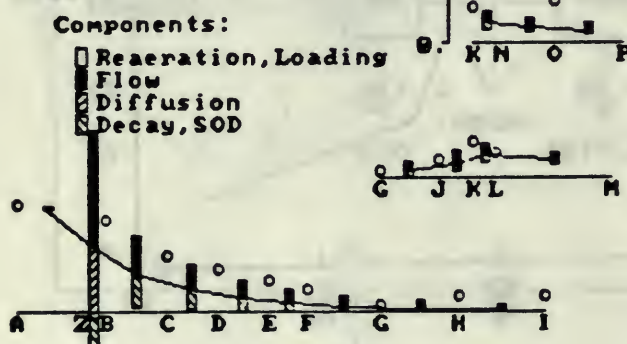
[DO] (MG/L)
top layer
Aug. 14 2400 hours
1986



[DO] (MG/L)
top layer
June 20 2400 hours
1987



[DO] (MG/L)
top layer
Aug. 15 2400 hours
1986



[DO] (MG/L)
top layer
June 21 2400 hours
1987

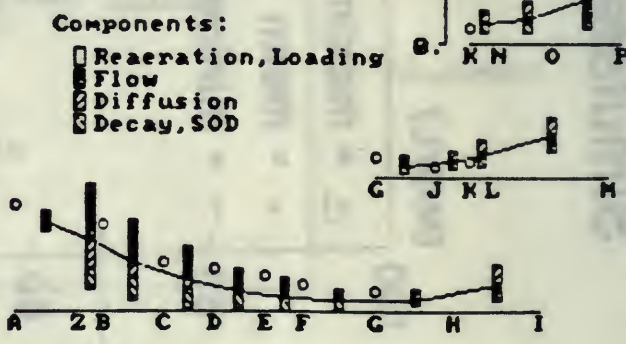
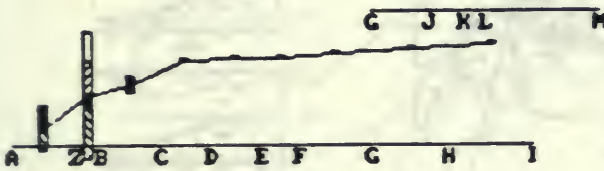
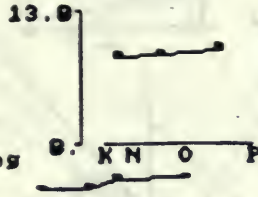


Figure 4. Simulated and Observed Top Layer DO

[DO] (MG/L)
bottom layer
Aug. 13 2400 hours
1986

Components:

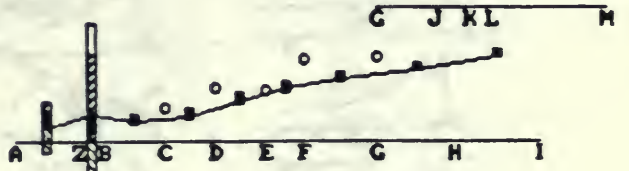
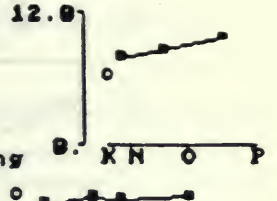
Reaeration, Loading
Flow
Diffusion
Decay, SOD



[DO] (MG/L)
bottom layer
June 19 2400 hours
1987

Components:

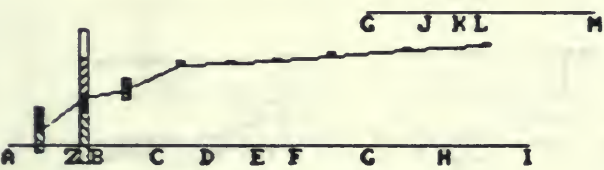
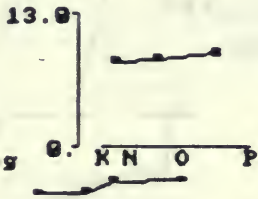
Reaeration, Loading
Flow
Diffusion
Decay, SOD



[DO] (MG/L)
bottom layer
Aug. 14 2400 hours
1986

Components:

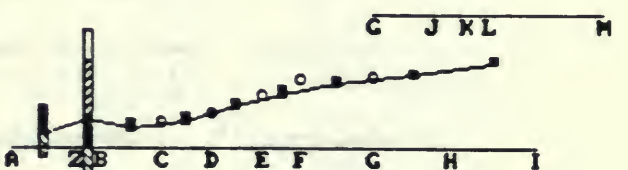
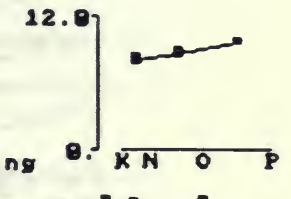
Reaeration, Loading
Flow
Diffusion
Decay, SOD



[DO] (MG/L)
bottom layer
June 20 2400 hours
1987

Components:

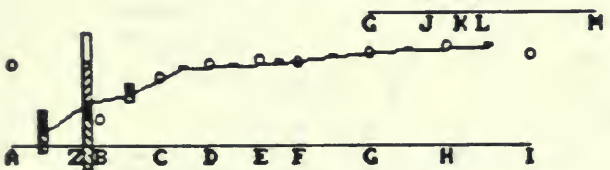
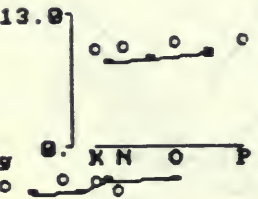
Reaeration, Loading
Flow
Diffusion
Decay, SOD



[DO] (MG/L)
bottom layer
Aug. 15 2400 hours
1986

Components:

Reaeration, Loading
Flow
Diffusion
Decay, SOD



[DO] (MG/L)
bottom layer
June 21 2400 hours
1987

Components:

Reaeration, Loading
Flow
Diffusion
Decay, SOD

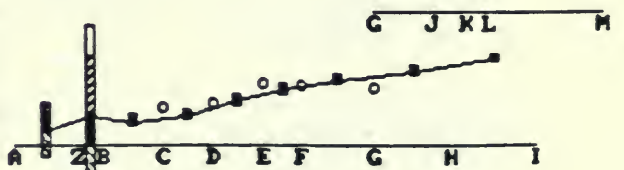
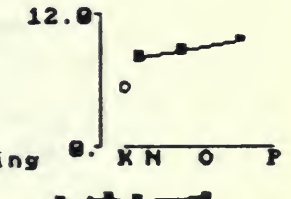


Figure 5. Simulated and Observed Bottom Layer DO

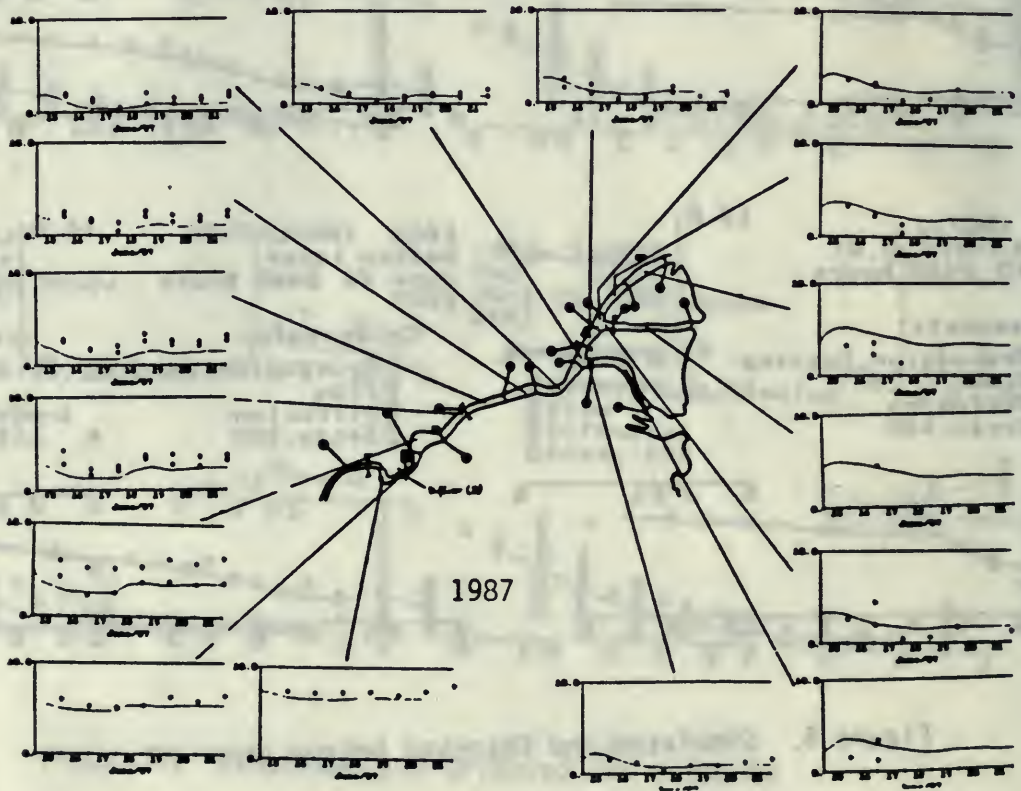
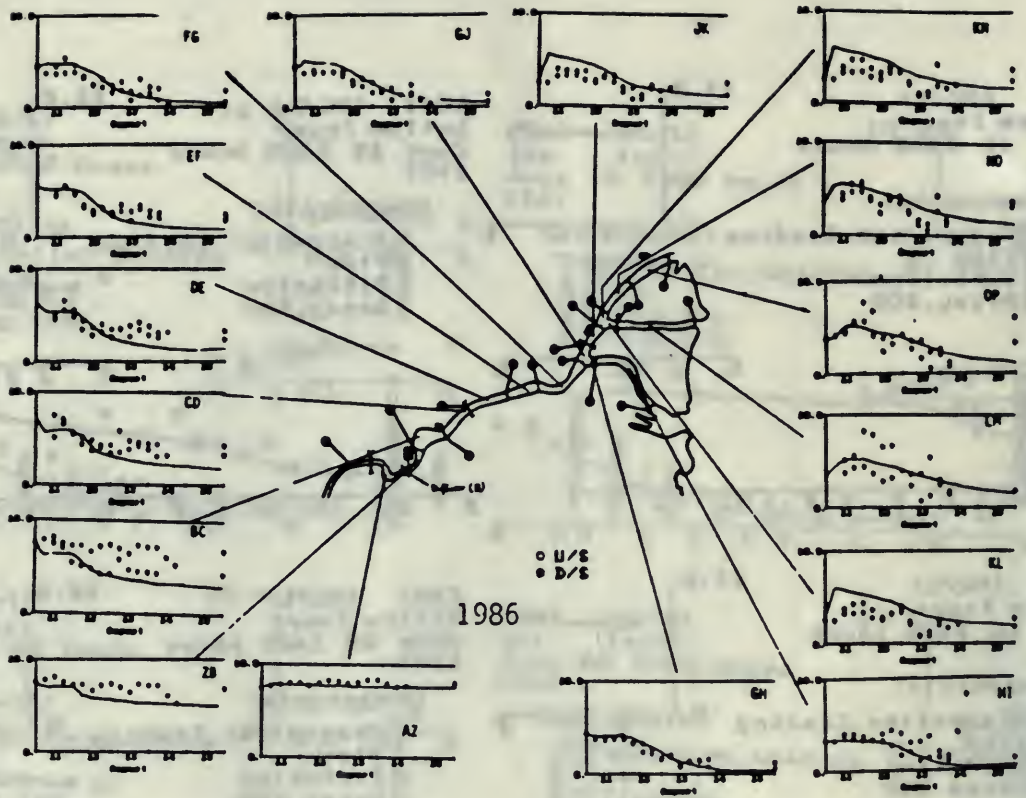


Figure 6. Time Series of Top Layer D0

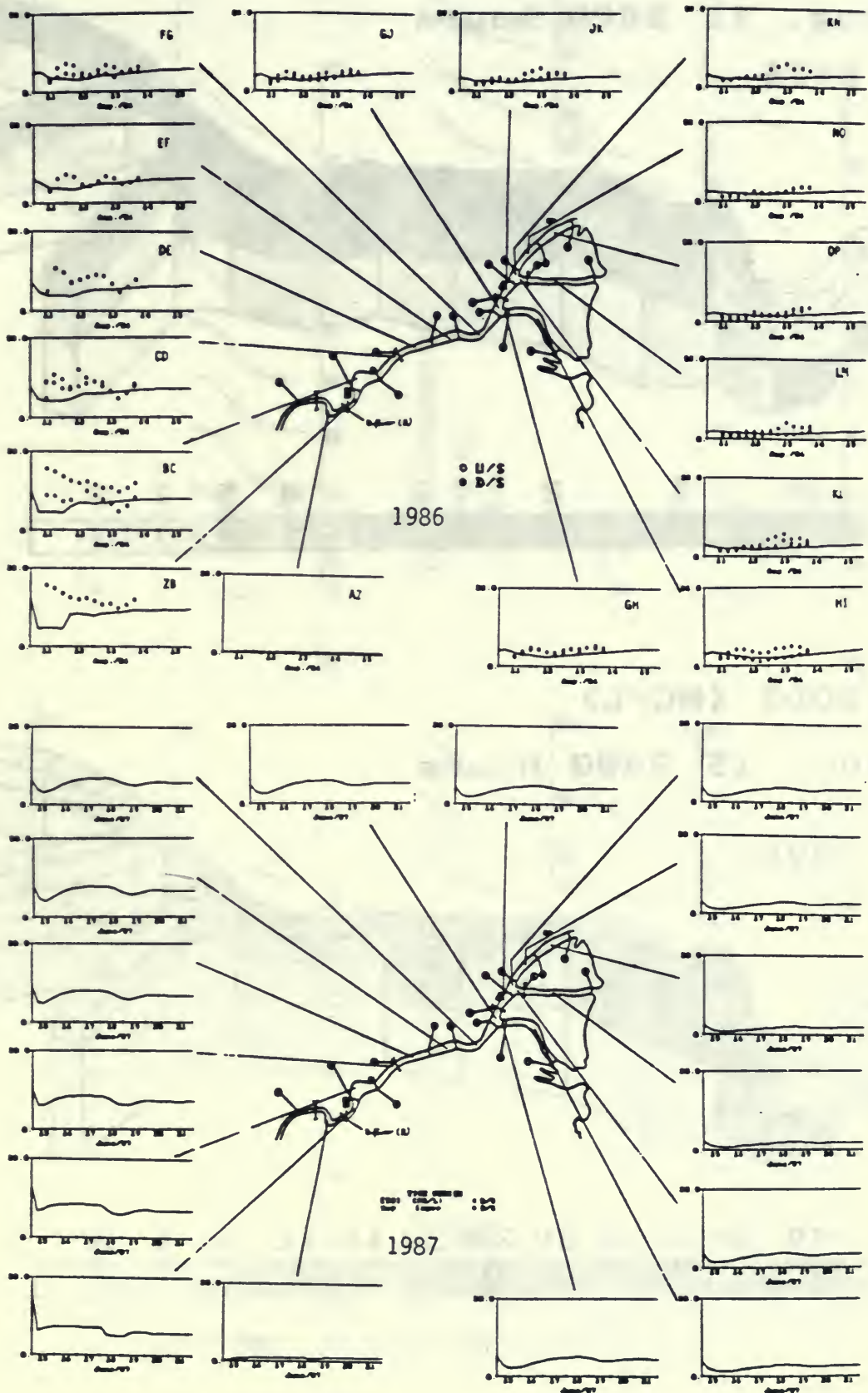
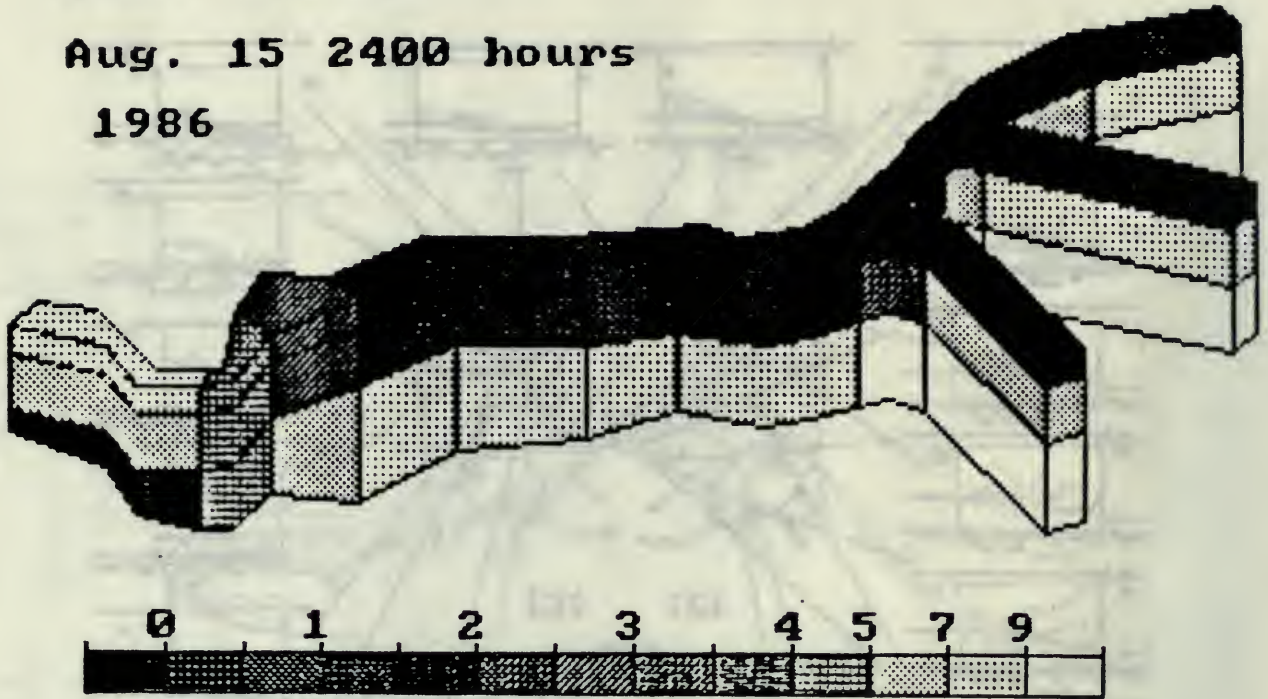


Figure 7. Time Series of Top Layer BOD

[DO] (MG/L)

Aug. 15 2400 hours

1986



[BOD] (MG/L)

Aug. 15 2400 hours

1986

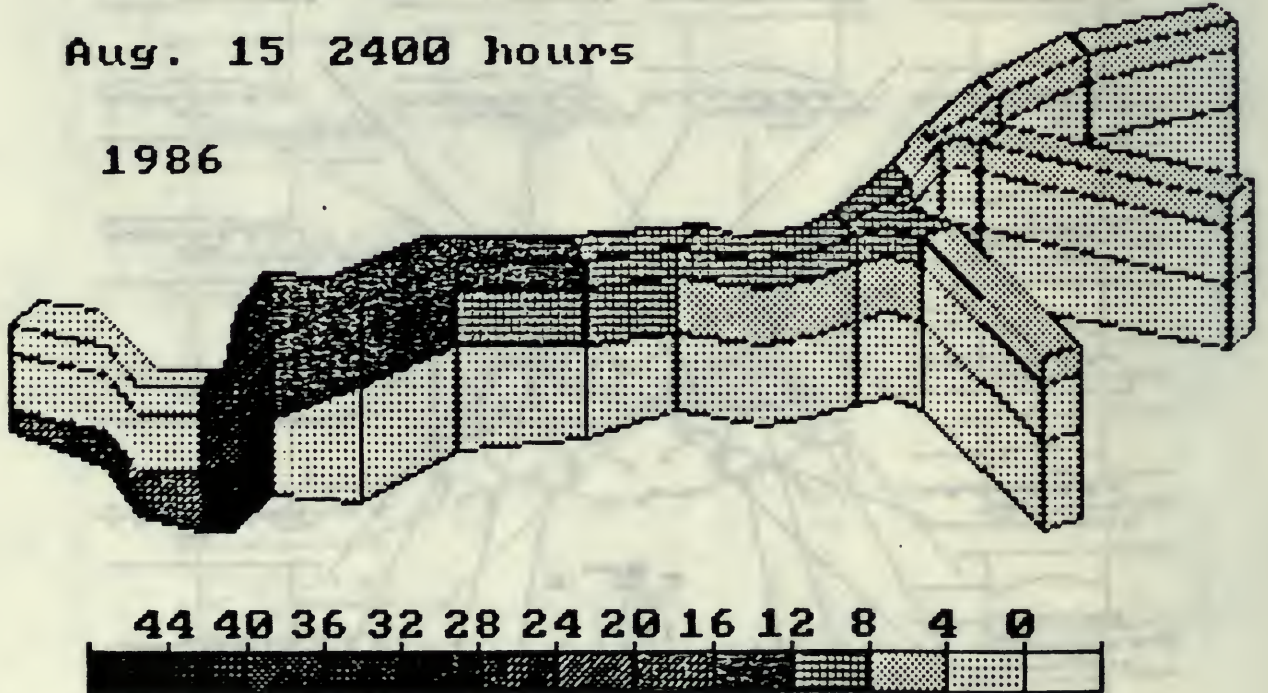
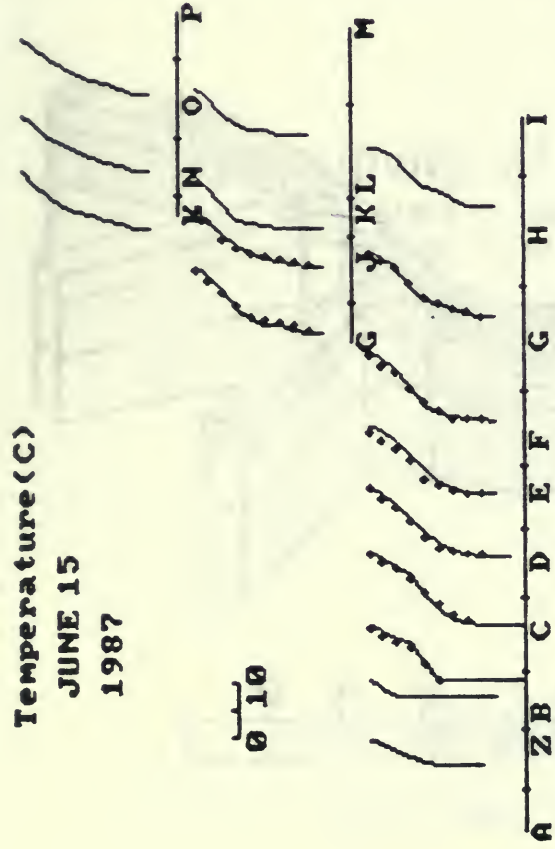
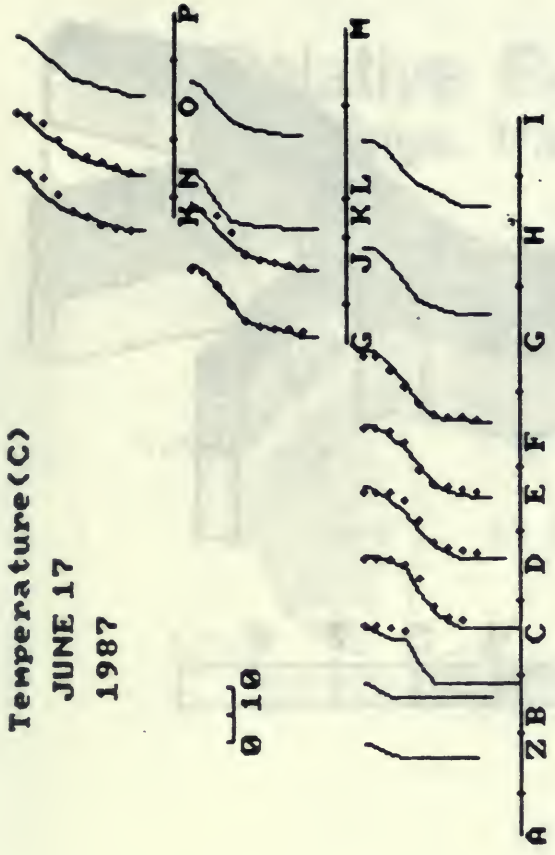


Figure 8. DO and BOD August 15, 1986 in 3-D

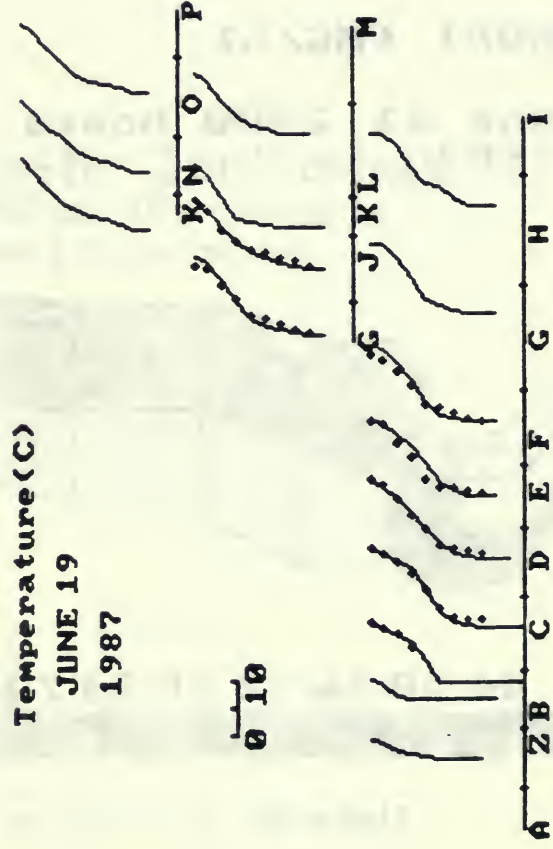
Temperature (C)
JUNE 15
1987



Temperature (C)
JUNE 17
1987



Temperature (C)
JUNE 19
1987



Temperature (C)
JUNE 21
1987

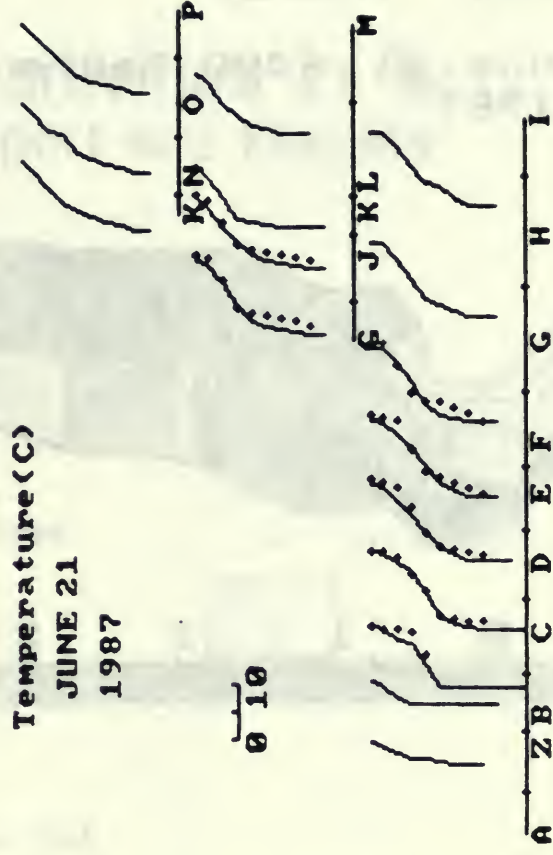
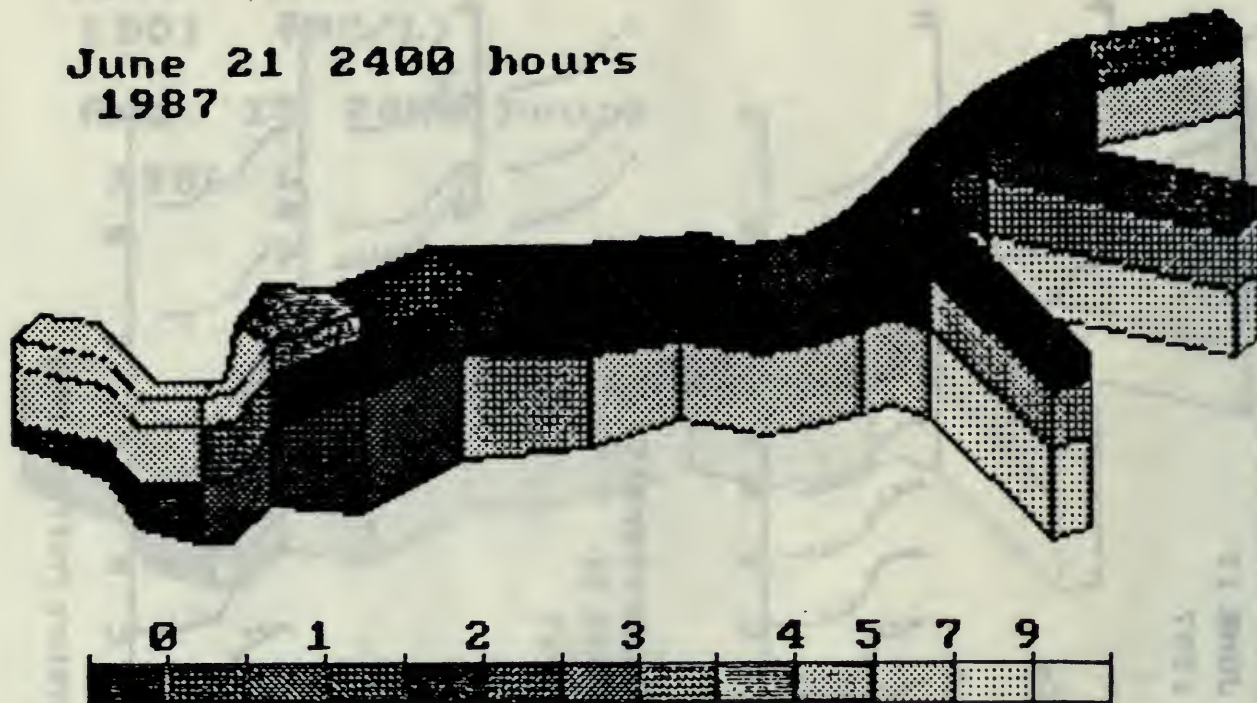


Figure 9. Simulated and Observed Temperature Profiles, 1987

[DO] (MG/L)

June 21 2400 hours
1987



[BOD] (MG/L)

June 21 2400 hours
1987

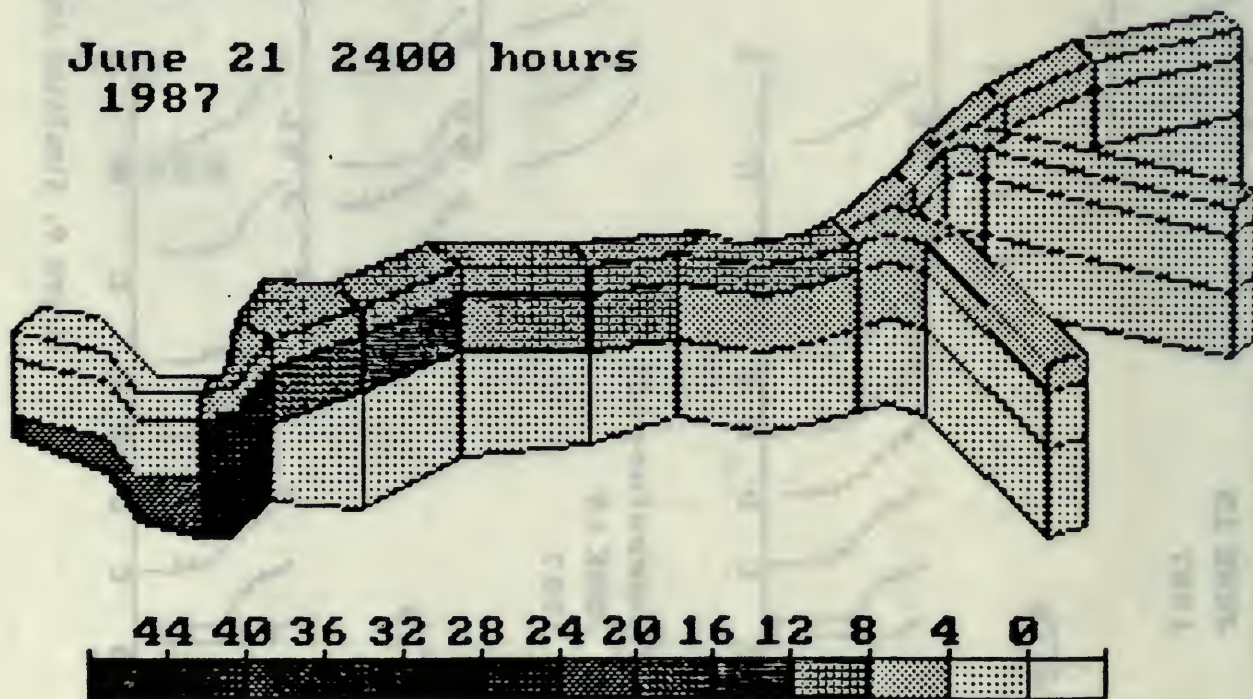


Figure 10. DO and BOD June 21, 1987 in 3-D

Relative Sensitivities in %: Loadings, transport and kinetics

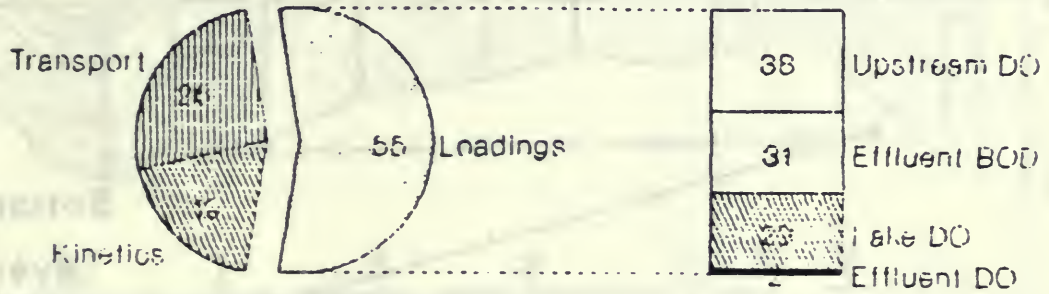


Figure 11(a).

Sensitivity of Kinetic Coefficients (% change in top [DO] for 40% change in kinetic coefficients in the model)

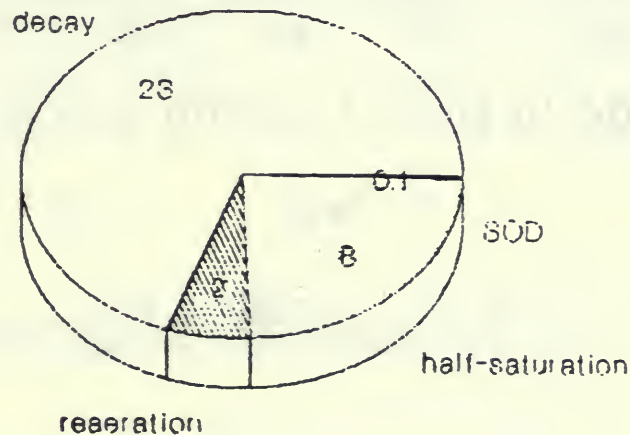


Figure 11(b).

Response of DO at GJ to BOD Loading Changes

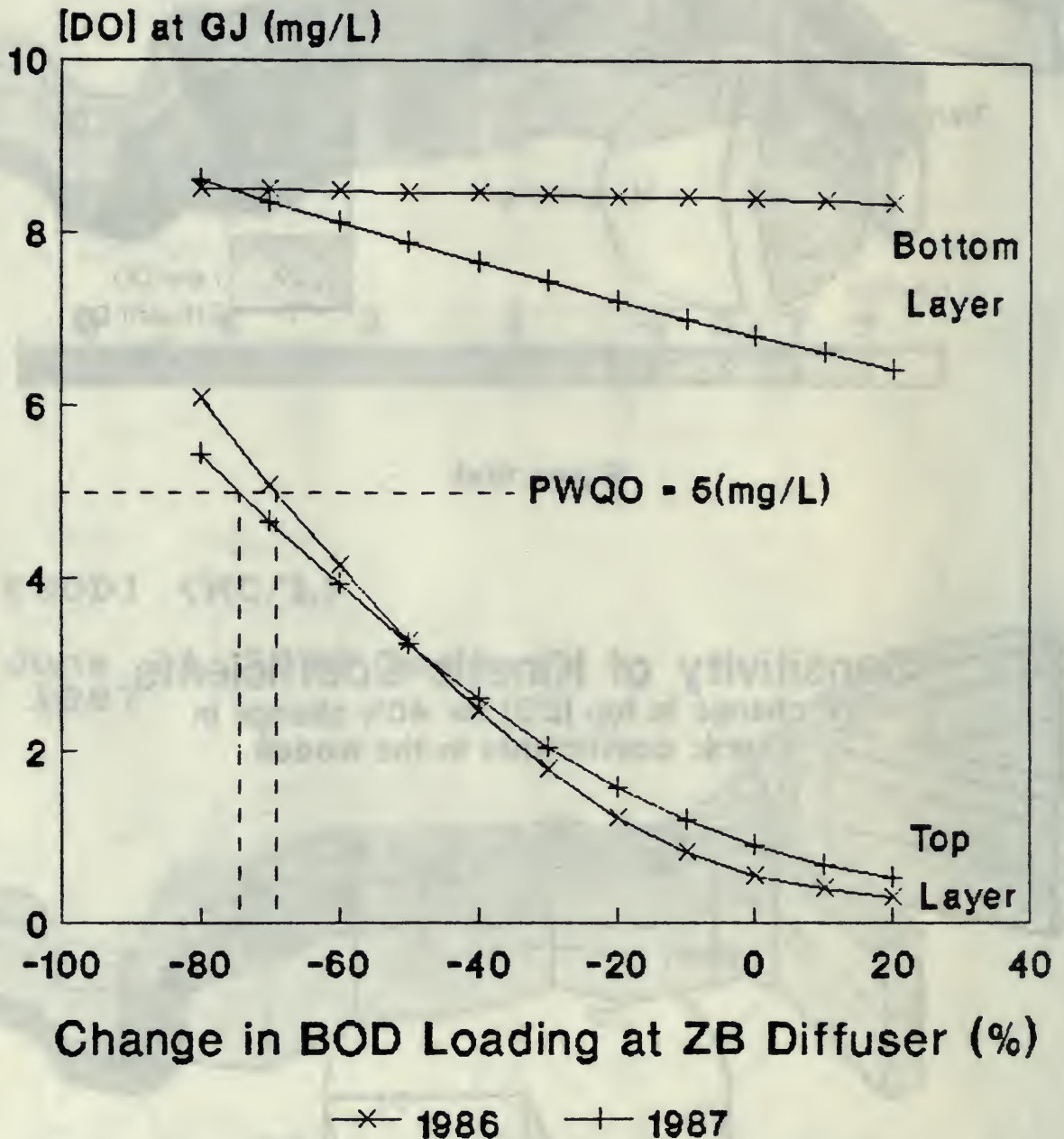


Figure 12

[DO] (MG/L)

June 21 2400 hours
1987

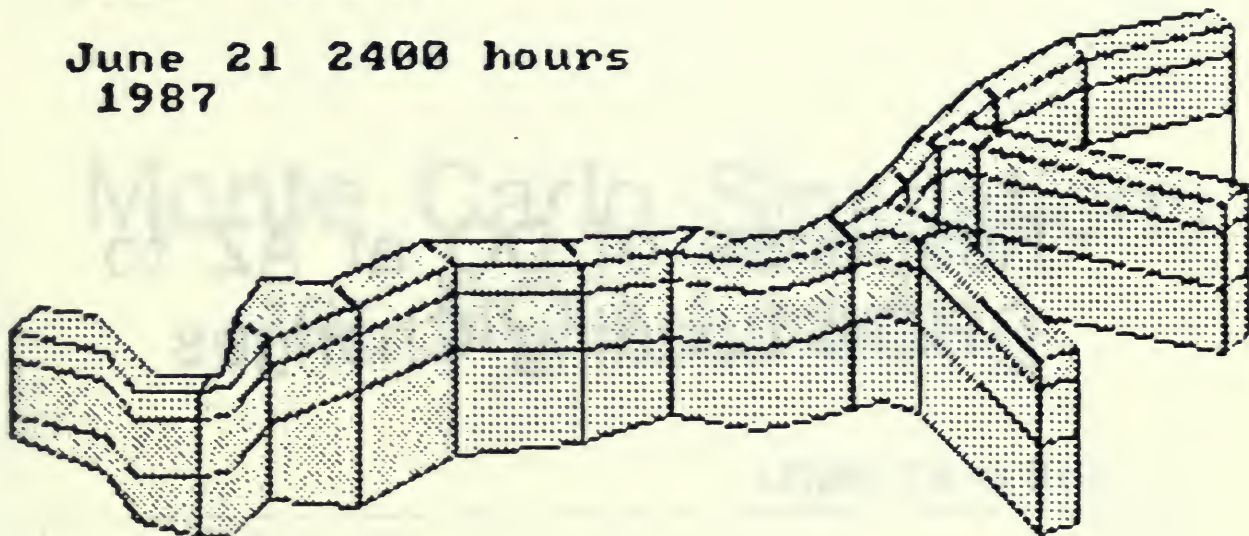


Figure 13. DO in 3-D June 21, 1987 with 80% BOD Load Reduction from ZB

[DO] (MG/L)

June 21 2400 hours
1987

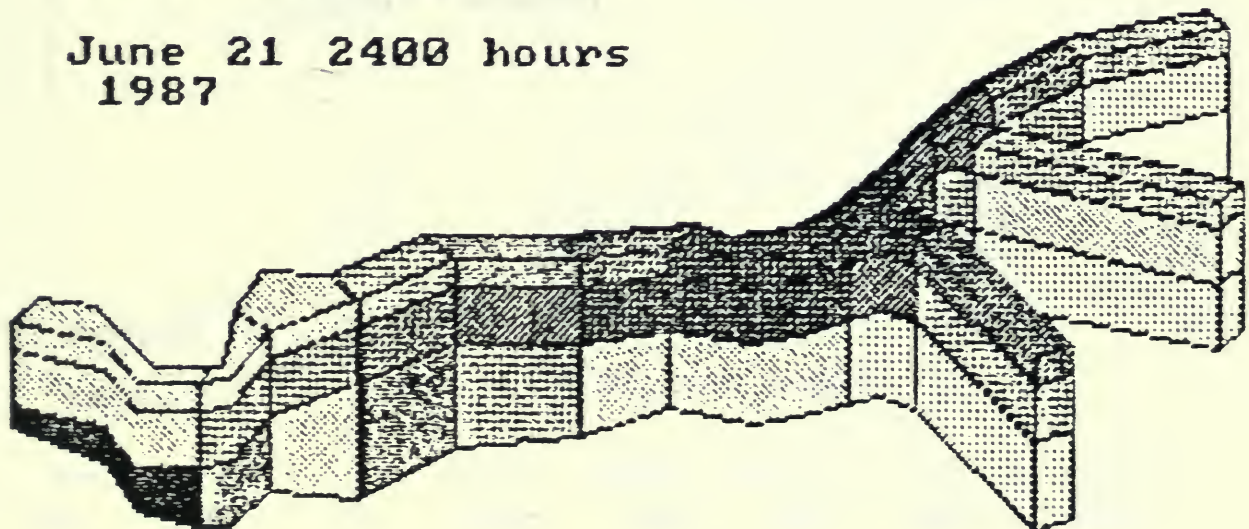


Figure 14. DO in 3-D June 21, 1987 with 10,000 kg/d DO Diffused into Segment BC

Response of DO at AZ to BOD Loading Changes

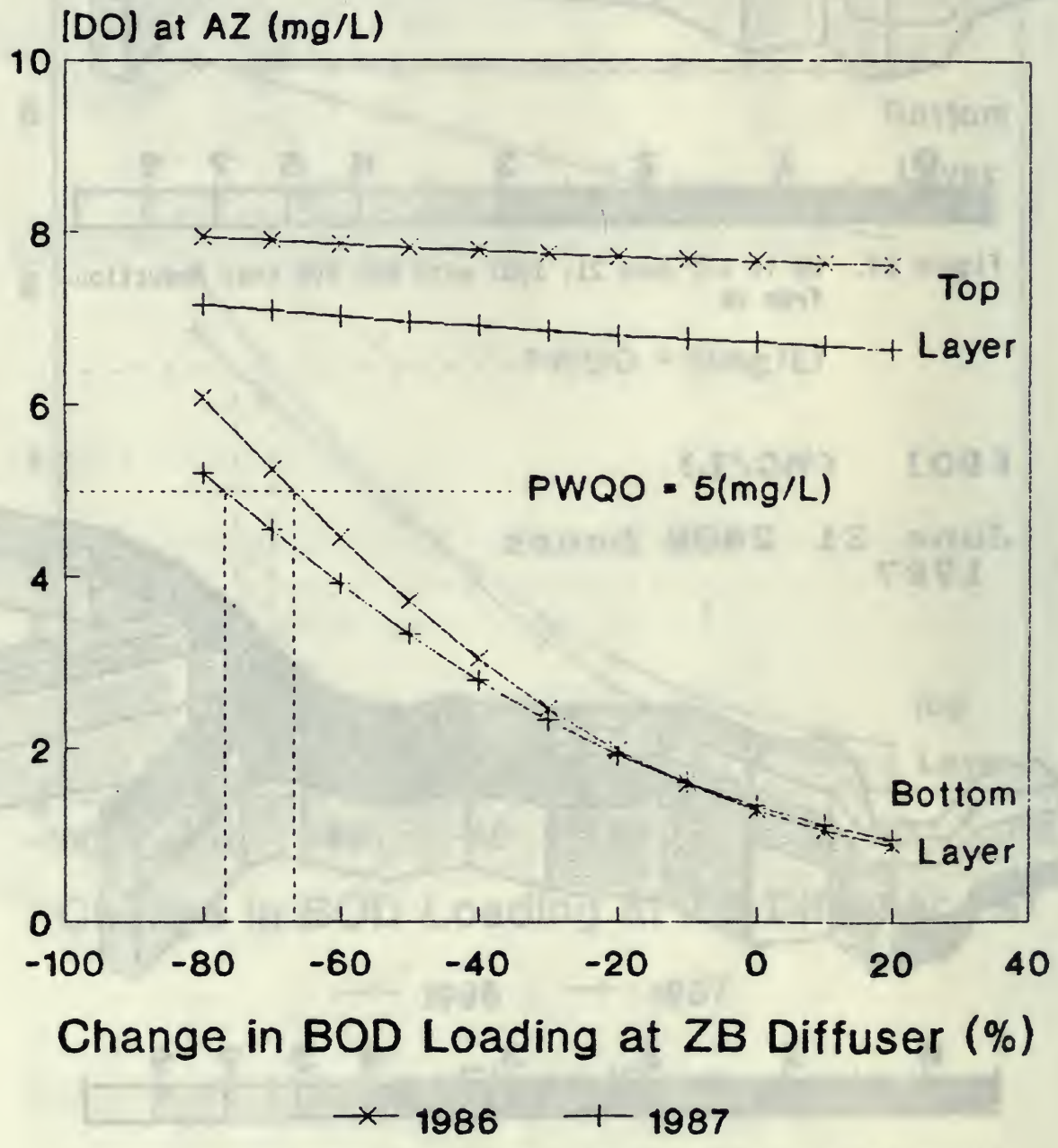


Figure 15

Monte Carlo Simulations for BOD Loading

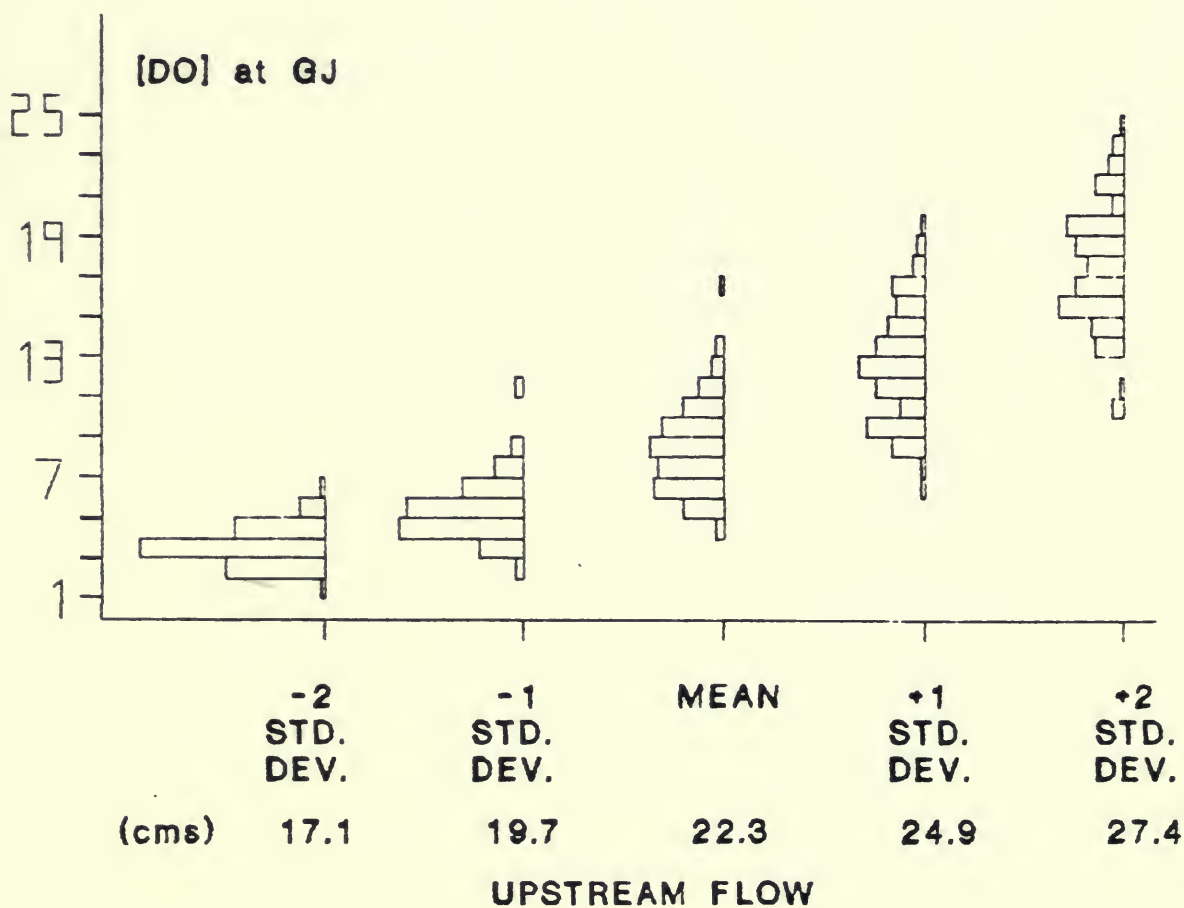
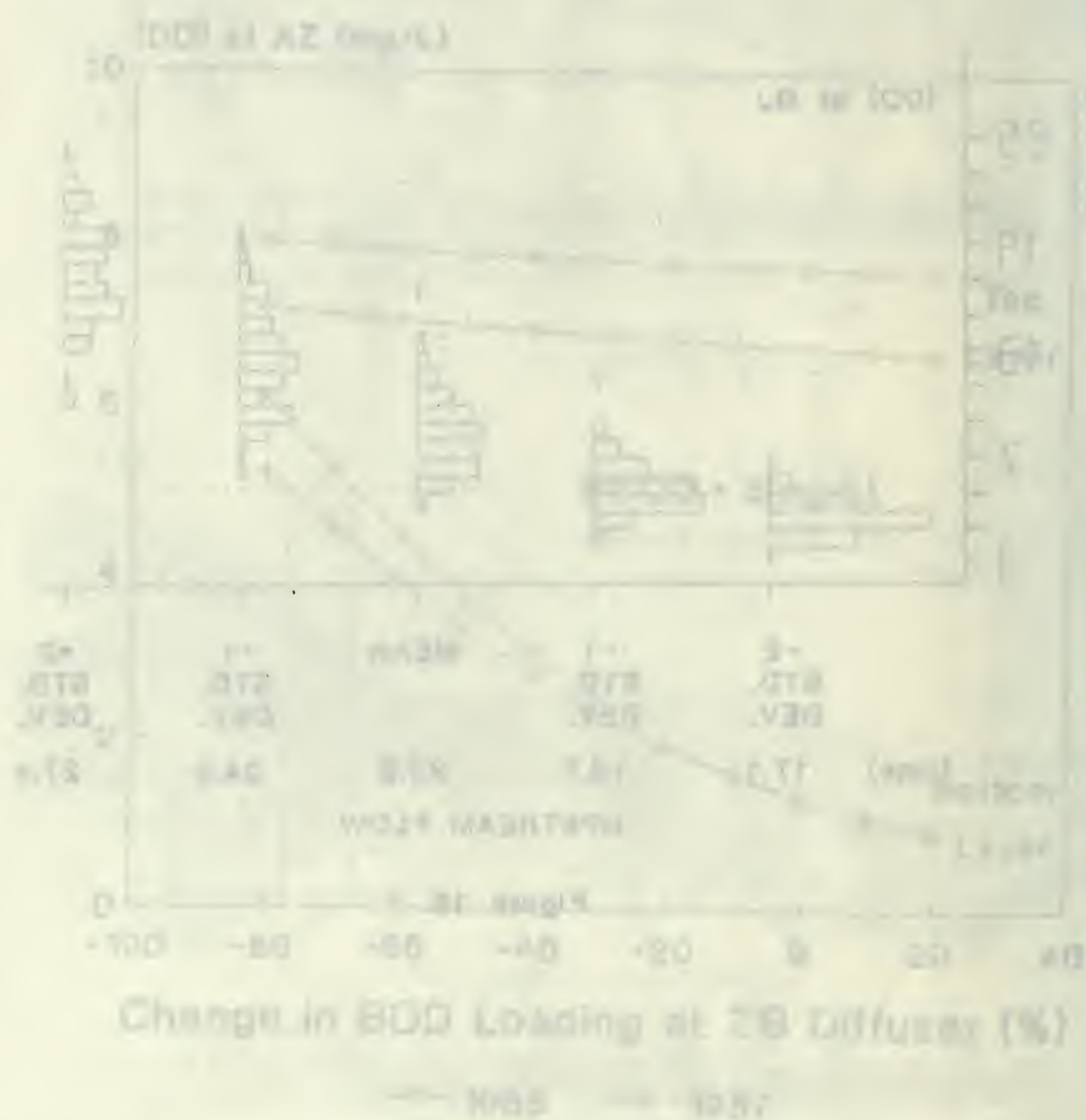


Figure 16.

Monte Carlo Simulations of AZ at 100 to 200 mg/L for BOD Loading



Change in BOD Loading at 28 Diffuser (%)

Figure 15

